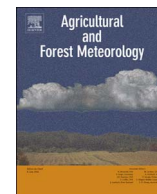




Contents lists available at ScienceDirect

## Agricultural and Forest Meteorology

journal homepage: [www.elsevier.com/locate/agrformet](http://www.elsevier.com/locate/agrformet)

## Water requirements of short rotation poplar coppice: Experimental and modelling analyses across Europe

Milan Fischer<sup>a,b,\*</sup>, Terenzio Zenone<sup>c</sup>, Miroslav Trnka<sup>a,d</sup>, Matěj Orság<sup>a,d</sup>, Leonardo Montagnani<sup>e</sup>, Eric J. Ward<sup>b,f</sup>, Abhishek Mani Tripathi<sup>a</sup>, Petr Hlavinka<sup>a,d</sup>, Günther Seufert<sup>g</sup>, Zdeněk Žalud<sup>d</sup>, John S. King<sup>b</sup>, Reinhart Ceulemans<sup>c</sup>

<sup>a</sup> Global Change Research Institute CAS, Bělidla 986/4a, 603 00, Brno, Czech Republic<sup>b</sup> Department of Forestry and Environmental Resources, North Carolina State University, Raleigh, NC 27695, USA<sup>c</sup> Department of Biology, Centre of Excellence on Plants and Ecosystems (PLECO), University of Antwerp, B-2610 Wilrijk, Belgium<sup>d</sup> Department of Agrosystems and Bioclimatology, Faculty of Agronomy, Mendel University in Brno, Zemědělská 1, 613 00 Brno, Czech Republic<sup>e</sup> Faculty of Science and Technology, Free University of Bolzano, Universitätsplatz 5, Piazza Università, I-39100 Bolzano, Italy<sup>f</sup> Climate Change Science Institute and Environmental Sciences Division, Oak Ridge National Laboratory, 1 Bethel Valley Road, Oak Ridge, TN 37830, USA<sup>g</sup> European Commission, DG-JRC, Institute for Environment and Sustainability, Climate Change Unit, Via Enrico Fermi 2749, T.P. 050, 21027 Ispra, VA, Italy

## ARTICLE INFO

## Keywords:

Bioenergy  
Bowen ratio and energy balance  
Crop coefficient  
Eddy covariance  
Evapotranspiration  
Water balance

## ABSTRACT

Poplars are among the most widely used short rotation woody coppice (SRWC) species but due to their assumed high water use, concerns have been raised with respect to large-scale exploitation and potentially detrimental effects on water resources. Here we present a quantitative analysis of the water requirements of poplar SRWC using experimental data and a soil water balance modelling approach at three different sites across Europe. We used (i) eddy covariance (EC) measurements (2004–2006) at an irrigated SRWC grown on a previous rice paddy in northern Italy, (ii) Bowen ratio and energy balance (BREB) measurements (2008–2015) and EC (2011–2015) at a SRWC in rain-fed uplands in the Czech Republic, and (iii) EC measurements (2010–2013) at a SRWC on a previous agricultural land with a shallow water table in Belgium. Without any calibration against water balance component measurements, simulations by the newly developed soil water balance model R-4ET were compared with evapotranspiration (ET) measurements by EC and BREB with a resulting mean root mean square error (RMSE) of 0.75 mm day<sup>-1</sup>. In general, there was better agreement between EC and the model (RMSE = 0.66 mm day<sup>-1</sup>) when EC data were adjusted for lack of energy balance closure. A comparison of the simulated and measured soil water content yielded a mean RMSE of 0.03 m<sup>3</sup> m<sup>-3</sup>. The mean annual crop coefficient, i.e. the ratio between actual and reference ET, was 0.82 (ranging from 0.65 to 0.95) while the monthly maxima reached 1.16. These values indicated that ET of poplar SRWC was significantly lower than ET of a well-watered grass cover at the annual time scale, but exceeded ET of the reference cover at shorter time scales during the growing season. We show that the model R-4ET is a simple, yet reliable tool for the assessment of water requirements of existing or planned SRWC. For very simple assessments on an annual basis, using a crop coefficient of 0.86 (adjusted to a sub-humid climate), representing an average value across the three sites in years with no evident drought stress, is supported by this analysis.

## 1. Introduction

Short rotation woody coppice (SRWC) cultures of *Populus* (poplars) and *Salix* (willows) are well known for high productivity, which make them suitable as bioenergy crops (Anderson et al., 1983; Isebrands and Richardson, 2014; King et al., 2013). To ensure high SRWC yields, a sufficient water supply is required (Deckmyn et al., 2004; Kim et al., 2008). Maintaining a favorable soil water balance typically relies on

adequate and well-distributed precipitation or on access to a shallow water table, which in turn requires careful site selection (King et al., 2013; Lindroth and Båth, 1999; Trnka et al., 2016). In most cases, irrigation of SRWC is economically inefficient and environmentally unsustainable (Kim et al., 2008; Persson, 1997). Moreover, bioenergy is a low-input commodity and any increase of (energy) inputs and carbon footprint inherently linked with intensive management, is undesirable (Djomo et al., 2011; Fischer et al., 2017; King et al., 2013).

\* Corresponding author at: Global Change Research Institute CAS, Zemědělská 1, Brno, 613 00, Czech Republic.  
E-mail address: [fischer.m@czechglobe.cz](mailto:fischer.m@czechglobe.cz) (M. Fischer).

<https://doi.org/10.1016/j.agrformet.2017.12.079>

Received 24 April 2017; Received in revised form 6 November 2017; Accepted 2 December 2017  
0168-1923/ © 2017 Elsevier B.V. All rights reserved.

**Nomenclature**

AWB	Above-ground woody biomass
BE	Belgium
Bowen adj.	Post closure scenario with energy residuum assigned to both turbulent energy fluxes according to Bowen ratio
BREB	Bowen ratio and energy balance
CP	Closed path
CZ	the Czech Republic
EC	Eddy covariance
EP	Enclosed path
ET	Actual evapotranspiration ( $\text{mm day}^{-1}$ )
$ET_0$	Reference evapotranspiration ( $\text{mm day}^{-1}$ )
FAO-56	Food and Agriculture Organization of the United Nations guidelines for computing crop water requirements
$F_r$	Stomatal resistance correction factor
$G$	Soil heat flux ( $\text{W m}^{-2}$ )
$h$	Mean stand height (m)
$H$	Sensible heat flux ( $\text{W m}^{-2}$ )
H adj.	Post closure scenario with energy residuum assigned only to $H$
IT	Italy
$K_c$	Crop coefficient
$K_{cb}$	Basal crop coefficient
$K_{cb \text{ full}}$	Basal crop coefficient of fully developed canopy
$K_{cb \text{ h}}$	Basal crop coefficient estimated from mean stand height
$K_{c \text{ min}}$	Minimum crop coefficient
$K_e$	Soil evaporation coefficient
$K_{SAT}$	Saturated hydraulic conductivity ( $\text{mm day}^{-1}$ )
LAD	Leaf area duration (days)
LAI	Leaf area index ( $\text{m}^2 \text{m}^{-2}$ )
LE	Latent heat flux ( $\text{W m}^{-2}$ )
LE adj.	Post closure scenario with energy residuum assigned only to LE

ME	Mean error
$n$	Number of observations
NSE	Nash–Sutcliffe model efficiency coefficient
OP	Open path
$p$	Crop specific stress parameter adjusted to actual reference evapotranspiration
$P$	Precipitation (mm)
$P.$	<i>Populus</i>
$p_{\text{tab}}$	Crop specific stress parameter at reference evapotranspiration of $5 \text{ mm day}^{-1}$
PAI	Plant area index ( $\text{m}^2 \text{m}^{-2}$ )
$r$	Stomatal resistance ( $\text{s m}^{-1}$ )
R-4ET	R-package for Empirical Estimate of Ecosystem EvapoTranspiration
$R^2$	Coefficient of determination
$R_G$	Incoming short-wave radiation ( $\text{W m}^{-2}$ )
$R_n$	Net radiation ( $\text{W m}^{-2}$ )
$RH_{\text{min}}$	Minimum daily air relative humidity (%)
RMSE	Root mean square error
SRWC	Short rotation woody coppice
SWC	Soil water content ( $\text{m}^3 \text{m}^{-3}$ )
$T_a$	Air temperature ( $^{\circ}\text{C}$ )
$u_2$	Wind speed measured at 2 m above ground ( $\text{m s}^{-1}$ )
WAI	Wood area index ( $\text{m}^2 \text{m}^{-2}$ )
WUE	Water use efficiency ( $\text{g kg}^{-1}$ )

**Greek letters**

$\Delta$	Slope of saturation vapor pressure curve ( $\text{kPa } ^{\circ}\text{C}^{-1}$ )
$\gamma$	Psychrometric constant ( $\text{kPa } ^{\circ}\text{C}^{-1}$ )
$\lambda$	Latent heat of vaporization ( $\text{J kg}^{-1}$ )
$\theta_{FC}$	Water content at the field capacity ( $\text{m}^3 \text{m}^{-3}$ )
$\theta_{SAT}$	Saturated water content ( $\text{m}^3 \text{m}^{-3}$ )
$\theta_{WP}$	Water content at the permanent wilting point ( $\text{m}^3 \text{m}^{-3}$ )

From an ecological perspective, the high water use reputation of poplars and willows is related to their natural habitats near streams, water bodies or wet areas (Isebrands and Richardson, 2014; Stanturf et al., 2001). High water requirements of poplars and willows, exceeding those of traditional crops (Deckmyn et al., 2004), grasslands (Persson, 1997) and forests (Grip et al., 1989), have been reported. Consequently, some concerns have been raised with regards to the economic (Lindroth and Båth, 1999) and ecological sustainability (Hall et al., 1996, 1998; Petzold et al., 2010) of SRWC cultures. It has been hypothesized that the large scale production of SRWC could potentially have detrimental effects on aquifers (Perry et al., 2001) and could decrease the water availability of the agricultural landscape (Hall et al., 1996, 1998). A recent review (Fischer et al., 2013b) showed that some studies (Bungart and Hüttel, 2004; Linderson et al., 2007; Migliavacca et al., 2009) have relatively low  $ET$ , contrary to fears about exceedingly high SRWC water use. This was recently supported by other studies (Bloemen et al., 2017; Fischer et al., 2015; Schmidt-Walter et al., 2014; Zenone et al., 2015) showing that  $ET$  of SRWC is lower than reference evapotranspiration ( $ET_0$ ) – i.e.  $ET$  of so called “reference grass” which is a typical reference vegetation cover characterized by no nutrient or soil water limitation (Allen et al., 1998). This may imply that water use of SRWC differs little from traditional, highly productive agricultural cropping systems (Fischer et al., 2013b; Horemans et al., 2017). Therefore, SRWC should not be limited by water availability if precipitation matches or exceeds  $ET_0$  at annual time scales, assuming an even temporal distribution of precipitation and/or soils with good water holding capacity (Fischer et al., 2013b).

The ratio between actual crop  $ET$  and  $ET_0$ , the crop coefficient ( $K_c$ ), is a traditional agricultural metric indicating crop water requirements

(Allen et al., 1998; Sánchez et al., 2012). It represents a core parameter in the agricultural water balance (Hlavinka et al., 2011; Raes et al., 2009; Rosa et al., 2012; Steduto et al., 2009) and in crop growth models (Brisson et al., 2003; Hlavinka et al., 2015; Liang et al., 2016). The Food and Agriculture Organization of the United Nations guidelines for computing crop water requirements (FAO-56) contains an exhaustive list of agricultural crop  $K_c$  values (Allen et al., 1998). For those crops for which  $K_c$  is not available (such as poplar), an estimate from plant height, ground cover, or leaf area index (LAI) can be applied (Allen et al., 1998).

Among the various studies on SRWC  $ET$ , only a few were explicitly focused on  $K_c$  (Fischer et al., 2013b). Moreover, caution is needed when applying some of the reported  $K_c$  values for upscaling and/or land-use management planning, since they were developed for very specific conditions. Early studies focused on intensively managed willows (mostly irrigated and fertilized) in Sweden, and  $K_c$  was derived by relating the measured or modeled  $ET$  to Penman (1948) potential evaporation (Persson, 1997; Persson and Lindroth, 1994). Sap flow based transpiration of poplars and willows in relation to  $ET_0$  was investigated during one abnormally hot and dry summer in southwest England (Hall et al., 1998). A more recent lysimetric study on poplars and willows from Italy was less representative for agricultural field conditions since  $ET$  measurements were carried out in a phytoremediation system with strikingly high  $ET$  and  $K_c$  values (Guidi et al., 2008). Finally, extremely arid conditions in a study from northwest China (Hou et al., 2010) precludes wider extrapolation of poplar  $K_c$  to common agricultural systems. The available literature on  $ET$  of poplars and willows was reviewed (Fischer et al., 2013b) and local experimental data were combined with long-term regional estimates of  $ET_0$  (Droogers and Allen,

2002). This analysis suggested that the average  $K_c$  of poplars and willows at an annual timescale was 0.8–0.9. From these and other findings, it was proposed that  $ET_o$  could serve as a rough estimate of SRWC  $ET$  if water availability is not a limiting factor. Experimental evidence from Germany confirmed that  $K_c$  of poplars was around 1.0 on rainless days throughout the main growing season (Schmidt-Walter et al., 2014), which was recently supported by experimental and modelling results from a multi-genotype poplar SRWC in Belgium (Bloemen et al., 2017; Horemans et al., 2017).

To provide a robust  $K_c$  parameter representative of commercial poplar SRWC covering different climatic, hydrological and soil conditions, we investigated measured and modeled  $ET$  at three different sites across Europe. To extend the previous suggestion of using  $ET_o$  as the SRWC  $ET$  proxy in areas where rainfall exceeds  $ET_o$  (Fischer et al., 2013b), we examined whether  $ET$  of poplars can be simulated using the FAO-56 methodology proposed for “not-listed crops”. To test this, we used a newly developed water balance model, R-4ET (Fischer et al., 2018), following the fundamental principles of the FAO-56 methodology and compared outputs with  $ET$  and soil water content measurements.

## 2. Materials and methods

Experimental data from three operational poplar SRWC plantations at different locations in Europe were used in this study: (i) Vigevano in northern Italy; (ii) Domaníněk in the Bohemian-Moravian Highlands, Czech Republic; and (iii) Lochristi in Flanders, Belgium.

### 2.1. Vigevano site (Italy)

The Vigevano site is located in the basin of the Ticino river in north-west Italy (Table 1). The plantation occupies a flat area of 80 ha. The climate of the site is classified as temperate with hot and dry summers (Peel et al., 2007). The topsoil originated from fluvial sediments with a sandy-loam texture. The area was previously managed for agricultural cultivation (rice and corn rotations) representing the typical land use of the region. The SRWC was established in March 2004, using hardwood cuttings (*Populus generosa* × *P. nigra*, clone Pegaso) in a double-row design with a spacing of  $2.8 \times 0.75 \times 0.45$  m corresponding to a planting density of 12,500 trees  $\text{ha}^{-1}$ . After planting, a pre-emergent herbicide was applied to prevent weed competition. In spring and summer 2004, four additional mechanical weed controls were applied. In the second and third year of cultivation, the management was limited to mechanical weed control in spring and at the beginning of summer. During the growing season, from May to September of all years, the plantation was irrigated using the basin method with a water volume of  $\sim 1500 \text{ m}^3 \text{ ha}^{-1}$  (precipitation equivalent of 150 mm). The plantation was harvested at the end of 2004 and 2006. The mean annual above-ground woody biomass (AWB) productivity during these three years was  $12.4 \text{ Mg ha}^{-1} \text{ y}^{-1}$  (Zenone, 2007).

### 2.2. Domaníněk site (Czech Republic)

The Domaníněk site is located in a typical rain-fed area of the Bohemian-Moravian Highlands of the Czech Republic (Table 1). The climate is classified as humid continental (Peel et al., 2007). The soil is characterized as a deep luvic cambisol influenced by gleyic processes. Although the area does not provide optimal conditions for SRWC with poplar (mainly due to the relatively low precipitation of  $633 \text{ mm y}^{-1}$ ), the experimental site itself is highly suitable, due to a deep soil profile with good water holding capacity (Trnka et al., 2008). The site topography is characterized by rolling hills with gentle eastward slopes of 3–5°.

The operational high-density monoclonal poplar (*P. nigra* × *P. maximowiczii*, clone J-105) plantation was established over a total area of 2.85 ha in April 2002. The plantation was established on agricultural

land previously cropped predominantly for cereals and potatoes. Following conventional tillage practices, hardwood cuttings were planted in a double-row pattern with inter-row distances of 2.5 m and within-row spacings of  $0.7 \times 0.7$  m to produce a density of 10,000 trees  $\text{ha}^{-1}$ . In keeping with the anticipated low-input management of future SRWC cultures, no irrigation, no fertilization and no herbicide treatments were applied. Mechanical weeding was carried out two times per growing season until canopy closure in 2005. Due to the high weed competition, the first rotation period was prolonged to 8 years, and the first harvest was carried out at the end of 2009. The second harvest was conducted at the end of 2015. The mean annual AWB productivity during 2002–2015 was  $9.0 \text{ Mg ha}^{-1} \text{ y}^{-1}$  with an annual maximum about  $16.5 \text{ Mg ha}^{-1} \text{ y}^{-1}$  (Fischer et al., 2015).

### 2.3. Lochristi site (Belgium)

The Lochristi site is an operational multi-genotype poplar SRWC situated in the coastal plain of East Flanders, Belgium (Table 1). The area is characterized by a moderate oceanic climate (Peel et al., 2007) with precipitation of  $756 \text{ mm y}^{-1}$  evenly distributed over the year. The site is characterized by a very shallow water table with occasional periods when water is standing above the soil surface. Prior to the SRWC establishment, the site was an artificially drained intensively cultivated agricultural land (62% of the total surface area) sown by ryegrass, wheat, potatoes and beet. More recently, the land was cultivated with corn monoculture, regularly fertilized with N at a rate of  $200\text{--}300 \text{ kg ha}^{-1} \text{ y}^{-1}$  as liquid animal manure and chemical fertilizer. The remaining part (38% of the total area) was intensively grazed pasture. An area of 14.5 ha was planted at a density of 8,000 trees  $\text{ha}^{-1}$  on April 7–10, 2010, with 12 selected and commercially available poplar and three willow genotypes. No fertilizers and no irrigation were applied during the four years of the study (2010–2013). The soil was characterized by a sandy texture with a clay-enriched deeper soil layer and poor natural drainage. The C and N mass fractions of the two previous land-use types were significantly different in the upper 0–0.15 m soil layer, while no significant differences were found in the upper 0.9 m (Broeckx et al., 2012). The mean annual AWB productivity was  $4.0 \text{ Mg ha}^{-1} \text{ y}^{-1}$  during the first rotation (2010–2011) and  $12.2 \text{ Mg ha}^{-1} \text{ y}^{-1}$  during the second rotation (2012–2013) (Verlinden et al., 2015).

### 2.4. Evapotranspiration measurements

Evapotranspiration was measured by eddy covariance (EC) at all three sites, and by the Bowen ratio and energy balance (BREB) method in Domaníněk (Table 2). In Vigevano, the EC system consisted of an open path ( $EC_{op}$ ) infrared gas analyzer (IRGA) LI-7500 (Li-Cor, Lincoln,

**Table 1**

Synoptic overview of the site and stand characteristics of the three experimental sites. The long-term (1961–1990) averages of climatic data were obtained from global 30 arc-second ( $\sim 1 \text{ km}$ ) database (Hijmans et al., 2005).  $ET_o$  abbreviates the reference evapotranspiration.

Site	Vigevano	Domaníněk	Lochristi
Country	Italy (IT)	Czech Republic (CZ)	Belgium (BE)
Latitude (decimal °N)	45.3	49.52	51.11
Longitude (decimal °E)	8.88	16.24	3.85
Altitude (m above sea level)	105	530	6
Mean annual temperature (°C, 1961–1990)	12.7	7.0	10.3
Mean annual precipitation (mm, 1961–1990)	998	633	756
Mean $ET_o$ (mm, 1961–1990)	803	644	663
Year of stand establishment	2004	2002	2010

**Table 2**

Synoptic overview of the instruments, measurement infrastructure and methods used for evapotranspiration measurements at the three sites. Evapotranspiration was measured by eddy covariance method (EC) with either open path (EC<sub>OP</sub>), enclosed path (EC<sub>EP</sub>) or closed path (EC<sub>CP</sub>) infrared gas analyzer, and by Bowen ratio and energy balance method (BREB).

Site	Vigevano (IT)	Domaníněk (CZ)	Lochristi (BE)
Method	EC <sub>OP</sub>	BREB, EC <sub>OP</sub> and EC <sub>EP</sub>	EC <sub>CP</sub>
Period of operation used in this study	Jul-04 to Aug-06	BREB: May-08 to Dec-15 EC <sub>OP</sub> : Jun-11 to Dec-14 EC <sub>EP</sub> : Sep13 to Dec-15	Jun-10 to Dec-13
EC analyzer	LI-7500	LI-7500A and LI-7200	LI-7000
Sonic anemometer	Gill R3 HS	Gill Windmaster	CSAT3
EC software	MASE	EddyPro	EdiRe
EC sampling frequency (Hz)	10	20	10
Axis rotation for tilt correction	Double rotation	Double rotation	Double rotation
Time lag compensation	Covariance maximization	Covariance maximization	Covariance maximization
Density fluctuation correction	Webb et al. (1980)	Webb et al. (1980)	Webb et al. (1980)
Correction for high frequency loss	Moncrieff et al. (1997)	EC <sub>OP</sub> : Moncrieff et al. (1997) EC <sub>EP</sub> : Horst (1997)	Horst (1997)
Correction for low frequency loss	Moncrieff et al. (2004)	Moncrieff et al. (2004)	Moncrieff et al. (2004)
Quality check	3 flags – Mauder and Foken (2006)	3 flags – Mauder and Foken (2006)	9 flags – Foken and Wichura (1996)

NE, USA) and a sonic anemometer Gill R3 HS (Gill Instruments, Lymington, UK). The raw EC data were logged by a notebook computer at sampling frequency of 10 Hz and fluxes were computed using the MASE (Multi-Anemometer Eddy Software) developed in LabWindows/CVI (Manca, 2003). The height of the EC measurements was kept at ~2.5 m above the canopy.

For Domaníněk, the BREB measurements were previously described in detail (Fischer et al., 2013b). The BREB system consisted of net radiometer NR 8110 (Philipp Schenk GmbH Wien, Austria), soil heat flux sensor HFP01 (Hukseflux Thermal Sensors, Netherlands), and three air temperature/relative humidity sensors EMS33 (EMS Brno, Czech Republic) for measuring the Bowen ratio. In July 2013, the mast with the BREB system was replaced by a new system using EMS33R (EMS Brno, Czech Republic) instruments for air temperature/relative humidity. EC fluxes (Table 2) were measured by an EC<sub>OP</sub> consisting of LI-7500A IRGA (Li-Cor, Lincoln, NE, USA) and a Gill Windmaster sonic anemometer (Gill Instruments, Lymington, UK). This EC system was initially placed on the same mast as the BREB, but it was moved in April 2012, on a newly erected mast 3 m southward and 8 m eastward from the BREB mast. In September 2013, an additional EC system with an enclosed path (EC<sub>EP</sub>) IRGA LI-7200 (Li-Cor, Lincoln, NE, USA) and sonic anemometer Gill Windmaster was installed on the mast with BREB. The 20 Hz raw EC data were processed by the Eddy Pro 6.2.0 software (Li-Cor, Lincoln, NE, USA). Because the EC systems in Domaníněk were powered by solar panels, the measurements were typically performed during the period from early March to early December to capture the main growing season. Due to the limited fetch at the site (Fischer et al., 2013b) the EC<sub>OP</sub> and EC<sub>EP</sub> were kept 1.0–1.5 m above the top of the canopy, while the lowest BREB level was kept 0.2–0.5 m above the top of the canopy.

The EC measurements at the Lochristi site were previously described in detail (Zenone et al., 2015). The EC system consisted of a three-dimensional sonic anemometer CSAT3 (Campbell Scientific, Logan, UT, USA) and a closed-path differential IRGA LI-7000 (Li-Cor, Lincoln, NE, USA). The 10 Hz raw data were processed using the EdiRe software (R. Clement, University of Edinburgh, UK; [www.geos.ed.ac.uk/homes/jbm/micromet/EdiRe/](http://www.geos.ed.ac.uk/homes/jbm/micromet/EdiRe/)).

At all three sites, the EC and BREB fluxes of latent ( $LE$ ,  $W m^{-2}$ ) and sensible heat ( $H$ ,  $W m^{-2}$ ) were calculated with a time step of 30 min and standard corrections and quality control (Foken et al., 2012) were applied (Table 2). Because the EC measurements in general do not fully close the simplified energy balance equation  $R_n = H + LE + G$ , where  $R_n$  is net radiation and  $G$  is soil heat flux (Foken, 2008; Wilson et al., 2002), the energy budget closure was forced at each 30-min period according to three scenarios to provide range of possible  $ET$  (Ingwersen et al., 2015):

- I  $H$  adjustment ( $H$  adj.) – The entire lack of energy balance closure is assigned only to  $H$ . Note that  $ET_{H\text{ adj.}}$  is identical to  $ET$  as measured by EC (Ingwersen et al., 2011).
- II Bowen ratio adjustment (Bowen adj.) – The lack of energy balance closure is distributed to both  $H$  and  $LE$  according to the measured Bowen ratio  $H/LE$  (Twine et al., 2000).
- III  $LE$  adjustment ( $LE$  adj.) – The entire lack of energy balance closure is assigned to  $LE$  (Falge et al., 2005). Note that in this case  $H$  remains as measured by EC while  $LE$  (or  $ET$ ) increases proportionally to the percentage of energy balance residuum.

The gaps in the time series of the fluxes measured by EC (all three scenarios) and BREB were gap-filled using an R-package REdyProc following standard methodology (Falge et al., 2001; Reichstein et al., 2005). To obtain  $ET$  in mm of water column,  $LE$  was divided by the latent heat of vaporization ( $\lambda$  in  $J kg^{-1}$ ) as a function of air temperature,  $T_a$  ( $^{\circ}C$ ), following  $\lambda = 2.50110^6 - 2361 T_a$  (Shuttleworth, 2007).

## 2.5. Evapotranspiration simulations

The model R-4ET (R-package for Empirical Estimate of Ecosystem EvapoTranspiration) used for simulations of  $ET$  within our study is described in detail in a separate contribution (Fischer et al., 2018). The model R-4ET is based on the soil water balance concept (Allen et al., 2011a) where the inflow is represented by rainfall, snowmelt, irrigation, capillary rise and the outflow by  $ET$ , runoff and deep percolation. The evapotranspiration is split into transpiration, soil evaporation and evaporation of rain interception. The rain interception depends on the precipitation and canopy storage capacity (Persson and Lindroth, 1994). The separation of transpiration and soil evaporation is carried out using a dual  $K_c$  approach (Allen, 2000; Allen et al., 1998; Kool et al., 2014), where  $K_c$  is split into the so called basal crop coefficient ( $K_{cb}$ ) and the soil evaporation coefficient ( $K_e$ ). The first (i.e.  $K_{cb}$ ) is primarily representing  $K_c$  of transpiration and depends on  $LAI$ , shortwave radiation reflectance, and stomatal and aerodynamic resistances. The second (i.e. the  $K_e$ ) is related to the energy and water balances of the topsoil (Allen et al., 2011a, 1998; Sánchez et al., 2012), and is therefore also dependent on the amount of litterfall and its decomposition rate (Odhiambo and Irmak, 2012). For those crops for which any reliable  $K_{cb}$  is not available, its potential value assuming full ground cover (i.e.  $LAI > 3$ ) can be estimated from mean stand height ( $h$ , m) as (Allen et al., 1998)

$$K_{cbh} = \min(1 + 0.1h, 1.2). \quad (1)$$

To account for the fact that this relation, and all the  $K_c$  and  $K_{cb}$  listed in FAO-56 (Allen et al., 1998) were originally proposed for sub-humid climates with average minimum daily relative humidity ( $RH_{min}$ ) of 45%



and average wind speed at 2 m over grass ( $u_2$ ) of  $2 \text{ m s}^{-1}$ , a subsequent adjustment to site specific climatic conditions is necessary (Allen et al., 1998)

$$K_{cb \text{ full}} = K_{cb \text{ h}} + (0.04(u_2 - 2) - 0.004(RH_{\min} - 45))\left(\frac{h}{3}\right)^{0.3} \quad (2)$$

To account for undeveloped canopy foliage and for eventually different (compared to the reference grass) stomatal resistance it follows that (Allen et al., 1998)

$$K_{cb} = K_{c \text{ min}} + (F_r K_{cb \text{ full}} - K_{c \text{ min}})(1 - \exp(-0.7LAI)), \quad (3)$$

where  $K_{c \text{ min}}$  is the minimum  $K_c$  (assumed to be zero in our study) and  $F_r$  represents a resistance correction factor (Allen et al., 1998). Note, that the exponent in Eq. (3) does not only represent an average radiation extinction coefficient (Campbell, 1986), but also accounts for micro-scale advection of  $H$  from soil enhancing canopy transpiration (Allen et al., 1998). The stomatal resistance correction factor in Eq. (3) is given as (Allen et al., 1998)

$$F_r = \frac{\Delta + \gamma(1 + 0.34u_2)}{\Delta + \gamma\left(1 + 0.34u_2\frac{r}{100}\right)}, \quad (4)$$

where  $\Delta$  is slope of saturation vapor pressure curve ( $\text{kPa } ^\circ\text{C}^{-1}$ ),  $\gamma$  is psychrometric constant ( $\text{kPa } ^\circ\text{C}^{-1}$ ), and  $r$  the stomatal resistance of sunlit poplar leaves (assumed to be  $100 \text{ s m}^{-1}$ , King et al., 2013). The value of 0.34 results from constant aerodynamic properties and surface resistance of the reference grass, while 100 represents mean stomatal resistance of sunlit leaves of the reference grass. The stomatal resistance of poplar sunlit leaves, showing a certain amount of isohydrity (Schmidt-Walter et al., 2014; Zenone et al., 2015), is further adjusted for the effect of vapor pressure deficit (Oren et al., 1999). This adjustment results in an increase in  $r$  and thus decreased  $F_r$ ,  $K_{cb}$  and  $ET$  whenever midday vapor pressure deficit exceeds 1 kPa.

By subtracting the outflow and inflow water balance components within a root zone, the soil water content ( $SWC$ ,  $\text{m}^3 \text{ m}^{-3}$ ) is obtained. The  $SWC$  extractable by plants is then split into a fraction that can be depleted before moisture stress occurs and a fraction for which  $K_{cb}$  is adjusted a by soil water stress coefficient (0–1) reducing  $K_{cb}$  (and therefore  $ET$ ) proportionally to decreasing  $SWC$  (Allen et al., 1998). The

plant accessible  $SWC$  fraction extractable without suffering water stress is dependent on atmospheric evaporative demand as

$$p = p_{\text{tab}} + 0.04(5 - ET_o), \quad (5)$$

where  $p_{\text{tab}}$  is a crop specific constant set typically to 0.5 (Allen et al., 1998).

The model R-4ET is an open source software written in the R language. It operates at a daily time step and while it is conceptually similar to other water balance models as e.g. SoilClim (Hlavinka et al., 2011), AquaCrop (Raes et al., 2009), or SimDualKc (Rosa et al., 2012), several distinctions exists (Fischer et al., 2018). For instance, in contrast to SoilClim, dual  $K_c$  approach (Allen, 2000) and capillary rise (Raes and Deproost, 2003) are adopted in R-4ET. Unlike SoilClim and SimDualKc, the soil profile within R-4ET is composed from multiple layers. Similarly to SoilClim but contrary to SimDualKc and AquaCrop, snow (Trnka et al., 2010) and rain interception (Persson and Lindroth, 1994) submodules are implemented in R-4ET. By contrast to all three mentioned models, R-4ET accounts for a dynamic mulch effect due to decomposing litterfall (Odhiambo and Irmak, 2012) reducing soil evaporation, and for the stomatal response to vapor pressure deficit (Oren et al., 1999). The two main input categories include hydro-meteorological data and crop data. The hydro-meteorological daily input variables comprise  $ET_o$ , precipitation and irrigation daily totals,  $RH_{\min}$ , maximum and minimum  $T_a$ ,  $u_2$ , and daily depth of the water table. The crop data include  $LAI$ , plant area index ( $PAI$ ,  $\text{m}^2 \text{ m}^{-2}$ ),  $h$  and rooting depth. As the crop variables are typically not available daily, they needed to be interpolated into the daily time step. No calibration against the measured water balance components was carried out to test whether their variation and magnitude can be reasonably explained solely by meteorological drivers, measured  $LAI$ , rooting depth, and commonly available soil hydraulic parameters.

## 2.6. Ancillary measurements

All three sites were instrumented by standard meteorological sensors (Table 3). The data measured on site were used as inputs within EC and energy balance closure computations. However, for calculating  $ET_o$  and for model inputs (except precipitation), data from nearby meteorological stations were used. Firstly, it is preferable and recommended to

**Table 3**  
Overview of the ancillary hydro-meteorological measurements with the instruments or methods used.

	Vigevano (IT)	Domanínek (CZ)	Lochristi (BE)
Net radiation	CNR1: Kipp & Zonen, Delft, the Netherlands	NR 8110: Philipp Schenk GmbH Wien, Austria	CNR1: Kipp & Zonen, Delft, the Netherlands
Soil heat flux	NA	HFP01: Hukseflux Thermal Sensors, the Netherlands	HFT3: REBS Inc., Seattle, WA, USA
Soil heat storage	NA	NA	TCAV-L: Campbell Scientific, Logan, UT, USA
Solar radiation	CNR1: Kipp & Zonen, Delft, the Netherlands	EMS 11: EMS Brno, the Czech Republic	CNR1: Kipp & Zonen, Delft, the Netherlands
Air temperature and humidity	HMP45C: Vaisala, Helsinki, Finland	EMS 33: EMS Brno, the Czech Republic	HMP45C: Vaisala, Helsinki, Finland
Precipitation	ARG100: Campbell Scientific, Logan, UT, USA	MetOne 370: MetOne Instruments, USA	3665R: Spectrum Technologies Inc., Plainfield, IL, USA
Soil water content	TRIME-EZ: IMKO Micromodultechnik GmbH, Ettlingen, Germany	EC-10: Decagon Devices, Inc., USA <sup>a</sup>	CS616: Campbell Scientific, Logan, UT, USA
Depth of soil water content measurements (m)	0–0.11	0.1, 0.3, 0.9 <sup>a</sup>	0–0.1, 0–0.2, 0–0.3, 0.1, 0.2, 0.3, 0.4, 0.6, 1
Water table	NA	NA	PDCR1830: Campbell Scientific, Logan, UT, USA
Datalogger	DL2e: Delta-T Devices Ltd., Cambridge, UK	ModuLog 3029: EMS Brno, the Czech Republic	CR5000 and CR1000: Campbell Scientific, Logan, UT, USA
Location of the secondary meteorological station	Pavia, IT	Domanínek, CZ	Melle and Zelzate, BE
Distance of the secondary station from SRWC (km)	25	0.1	14 and 10

<sup>a</sup> Since 2014 replaced by CS616 (Campbell Scientific, Logan, UT, USA) with depths of 0.1, 0.25 and 0.5 m.

compute  $ET_0$  from data measured above short grass cover such as at standard meteorological stations (Allen et al., 1998). This is especially important in the case of wind speed, which differs inherently above these two aerodynamically distinct covers (SRWC versus reference grass). The surface differences can also play a role for temperature and humidity measurements, especially during the periods when SWRC is dominated by dry bare soil (e.g. during a dry spring). Secondly, the data from nearby meteorological stations provided a gap-free and consistent database. Precipitation was preferred from *in-situ* measurements due to the inherent spatial heterogeneity in precipitation. Daily precipitation was corrected to account for the wind induced underestimation determined from the rain gauge orifice height and wind speed (Yang et al., 1998). No measurements of  $G$  were available for Vigevano (Table 3) and therefore the following simple model parameterized in Lochristi ( $n = 62,875$ ,  $R^2 = 0.61$ ) was adopted

$$G = R_n 0.16 \exp(-0.27PAI) \text{ for } R_n \geq 0, \quad (6a)$$

$$G = R_n 0.53 \exp(-0.16PAI) \text{ for } R_n < 0. \quad (6b)$$

In Domanínek, no measurements of soil heat storage above the heat flux plate were carried out (Table 3). To avoid the resulting potential underestimation in the energy budget, we adopted a long-term average ( $n = 62,875$ ) value of  $G$  from Lochristi, being 1.6 times of the raw signal measured by the heat flux plates placed at 8 cm below the soil surface.

## 2.7. Leaf area index and stand height

In Vigevano,  $LAI$  (one-sided, projected) was determined using the LAI 2000 Plant Canopy Analyzer (PCA, Li-Cor Inc., Lincoln, NE). Data were collected biweekly throughout the growing season at five different plots across the field. Ten different sampling points were used along a transect of each plot covering both inter-rows and double-rows. Similarly, the  $LAI$  in Domanínek was measured on a weekly basis using a SunScan ceptometer system (Delta-T Devices Ltd., Cambridge, UK) while in Lochristi measurements were made biweekly via an LAI 2200 Plant Canopy Analyzer (PCA, Li-Cor Inc., Lincoln, NE). More details about the  $LAI$  measurements in Domanínek (Fischer et al., 2013b) and Lochristi (Broeckx et al., 2015; Vanbever et al., 2016) have been previously provided. At all three sites,  $LAI$  was calculated as the difference between  $PAI$  and wood area index ( $WAI$ ,  $m^2 m^{-2}$ ) with  $WAI$  determined during the dormant period. These optical, indirect  $LAI$  measurements were verified by destructive leaf collection at all three sites (Broeckx et al., 2015; Fischer, 2012; Zenone, 2007). Leaf area duration ( $LAD$ , days) at all three sites was determined as the period when  $LAI > 0$ . To ensure the continuous daily input data as required by the model,  $LAI$  was interpolated by applying the relationship between the cumulative heat sum ( $> 5^\circ C$ ) and the measured  $LAI$  (Linderson et al., 2007).

The mean stand height,  $h$ , at all sites was determined from site specific allometric equations between stem diameter and tree height obtained during the regular tree inventories at the end of each growing season. The change of  $h$  and  $WAI$  during the growing season was

assumed to be proportional to the cumulative heat sum ( $> 5^\circ C$ ) for the period from budburst until  $LAI$  decreased to half of the season maximum during senescence. Thereafter, wood growth was assumed to cease.

## 2.8. Assessments of rooting depth

The soil coring technique was used to determine fine root ( $\emptyset < 2$  mm) biomass. At each site, an 0.08 m diameter  $\times$  0.15 m deep hand-driven corer (Eijkelkamp, Giesbeek, the Netherlands) was used. In Vigevano, fine root profiles were obtained during sampling campaigns in July and December 2004, December 2005, and November 2006. A total of 90 soil cores up to a depth of 2 m were collected at each sampling campaign covering double-rows and inter-rows. In Domanínek, one sampling campaign was conducted in July 2013. In total, 60 core samples were collected up to a depth of 1.5 m. In Lochristi, rooting depth was determined from a 4-year long intensive belowground study described in detail elsewhere (Berhongaray et al., 2012, 2013, 2017).

For modelling purposes, an estimate of rooting depth at each day was required. In Vigevano root depth after planting was considered to increase proportionally to  $LAI$  (King et al., 2002) until it reached its final depth as determined by core sampling. In Domanínek, where the experiment started in the 7<sup>th</sup> year after planting, it was assumed that the root depth was constant. In Lochristi, it was assumed that the dynamics of root development depended on four factors: (i) maximum root depth, (ii) potential vertical root growth rate, (iii) presence of the water table, and (iv) tolerance of fine roots to flooding. The potential vertical growth rate was estimated from the Vigevano sequential root depth sampling in July 2004, and September 2004. New fine roots were assumed to be produced at the potential vertical growth rate in the drained area until maximum root depth or water table was reached. If the water table increased into the root zone during the growing season for more than 60 days (estimated fine root flooding tolerance), the submerged roots were assumed to become permanently inactive due to hypoxia (Broadfoot, 1973; Dickmann et al., 2001). New fine roots grew in that soil volume after the water table decreased. The effective depth of the root zone (i.e. the input depth for the model) at all three sites was considered 25% larger than the observed rooting depth to account for: (i) a potential allocation of roots into deeper layers under drought stress (Dickmann et al., 2001), and (ii) an assumption that due to soil water movement, there is typically no sharp transition of  $SWC$  between the root zone and the underneath soil layer.

## 2.9. Model parametrization and evaluation

The only site specific model parameters used were represented by soil parameters (Table 4) which were estimated from soil texture using pedotransfer functions (Rawls et al., 1982; Saxton et al., 1986; Williams and Ahuja, 1993). The remaining model parameters were considered generic and based on data available from the literature. The model simulations were validated by  $SWC$  and  $ET$  measurements. For  $SWC$ , an average  $SWC$  of the measured depth (Table 3) was compared with the average from identical depths simulated by the model. In the case of  $ET$ ,

**Table 4**

Site specific soil input parameters including hydraulic saturated conductivity ( $K_{SAT}$ ), water content at the field capacity ( $\theta_{FC}$ ), water content at the permanent wilting point ( $\theta_{WP}$ ), and saturated water content ( $\theta_{SAT}$ ).

Site	Vigevano (IT)				Domanínek (CZ)				Lochristi (BE)			
Depth (m)	0–0.3	0.3–0.6	0.6–1.1	1.1–3.0	0–0.2	0.2–0.3	0.3–0.6	0.6–3.0	0–0.2	0.2–0.5	0.5–0.9	0.9–2.0
No. of compartments	5	2	2	3	3	2	2	5	3	3	3	3
$K_{SAT}$ (mm day <sup>-1</sup> )	346	518	506	704	134	210	591	501	317	552	855	598
$\theta_{FC}$ (m <sup>3</sup> m <sup>-3</sup> )	0.31	0.24	0.24	0.28	0.32	0.30	0.31	0.33	0.25	0.23	0.22	0.25
$\theta_{WP}$ (m <sup>3</sup> m <sup>-3</sup> )	0.13	0.10	0.10	0.12	0.16	0.15	0.13	0.13	0.13	0.11	0.12	0.18
$\theta_{SAT}$ (m <sup>3</sup> m <sup>-3</sup> )	0.44	0.40	0.40	0.45	0.43	0.42	0.41	0.42	0.40	0.40	0.43	0.51
Soil class	sandy	sandy	sandy	sandy	loamy	loamy	loamy	loamy	sandy	sandy	sandy	sandy

the daily totals of measured  $ET$  were compared with the daily simulations. Within the integration of 30-min  $ET$  into daily totals, using of gap-filled values for the model comparison could not be avoided. To prevent any artefacts due to gap-filling, only those daily  $ET$  totals with less than 10% being gap-filled were considered. For validation of R-4ET simulations, we used standard error statistics (Willmott, 1982) including coefficients of determination ( $R^2$ ), mean error ( $ME$ ) and root mean square error ( $RMSE$ ). In addition, we used the Nash–Sutcliffe model efficiency coefficient ( $NSE$ ) which is widely applied in hydrology (Moriassi et al., 2007). This  $NSE$  can range from  $-\infty$  to 1. A  $NSE = 1$  corresponds to a perfect match of the simulations to the observed data. A  $NSE = 0$  indicates that the model simulations are as accurate as the mean of the observed data, whereas  $NSE < 0$  occurs when the observed mean is a better predictor than the model.

### 3. Results

#### 3.1. Weather conditions

Over the period of the observation, mean annual  $T_a$  in Vigevano was similar to the long-term average (1961–1990), whereas in the case of Domanínek and Lochristi the mean annual  $T_a$  was higher than the long-term normals (Table 5). In Vigevano, precipitation during the period 2004–2006 was more than 30% lower than the long-term mean, while it was similar in Domanínek and 20% higher in Lochristi as compared to the long-term averages (Table 5). The applied precipitation correction for the wind related rain-gauge underestimation (Yang et al., 1998) resulted on average in a 10% increase. The resulting corrected mean annual totals were 720 mm, 671 mm and 1021 mm for Vigevano, Domanínek and Lochristi, respectively. The mean evaporative demand of the atmosphere, expressed as  $ET_o$ , was the highest at Vigevano and the lowest at Domanínek (Fig. 1, Table 5). Although the lowest annual average solar radiation was observed in Lochristi, mean annual  $ET_o$  was slightly higher in Lochristi than in Domanínek mainly as a result of the higher  $u_2$ , lower  $RH_{min}$  and higher  $T_a$  (Table 5). The geographical differences resulted not only in different climatological averages, but also in different seasonal weather patterns. Most importantly, the length of the theoretical growing season (defined as the period when the mean daily  $T_a$  was continuously above  $5^\circ\text{C}$ ) was the longest in Vigevano (245 days), followed by Lochristi (225 days) and then Domanínek (172 days). The difference between the coastal and the continental climates was also obvious in  $ET_o$  during the dormant season when  $ET_o$  was the highest in Lochristi and the lowest in Domanínek (Fig. 1).

#### 3.2. Leaf area index, stand height and basal crop coefficient

The differences in the length of the theoretical growing season were caused by differences in phenology and therefore linked to the dynamics of  $LAI$  and differences in  $LAD$  (Fig. 2).  $LAD$  was on average the longest in Lochristi (218 days), followed by Vigevano (199 days), and the shortest in Domanínek (191 days). In Domanínek, after exclusion of the year 2010 with a late resprout after the harvest, the  $LAD$  was 198 days which did not change the ranking of the sites, but almost matched the  $LAD$  in Vigevano. The highest  $LAI$  was found in Domanínek with an average seasonal  $LAI$  maximum of 6.7 and an absolute  $LAI$

maximum of 8.3 in 2013. The seasonal  $LAI$  maxima averaged 4.0 and 3.1 in Vigevano and Lochristi, respectively.

As a result of the R-4ET model structure, a strong dependence of  $K_{cb}$  on measured  $LAI$  inherently exists (Eq. (3), Fig. 3). However, combination of stand height development (Eq. (1)), climatic conditions (Eq. (2)), aerodynamic resistance (Eq. (2)), and stomatal control (Eqs. (3) and (4)) resulted in a certain amount of variation in the  $K_{cb}$  to  $LAI$  relationship. The differences in measured  $h$ ,  $RH_{min}$  and  $u_2$ , caused that the  $K_{cb}$  to  $LAI$  curves differed from the reference sub-humid  $K_{cb}$  line (determined for  $u_2 = 2 \text{ m s}^{-1}$  and  $RH_{min} = 45\%$ ) as well as from site to site (Fig. 3).

By comparing the actual  $K_{cb}$  to the  $K_{cb}$  for sub-humid climate conditions, an integrative effect of different climatic conditions, stand height and stomatal control was quantified (Fig. 3). In general, all three sites were characterized by higher  $RH_{min}$  (Table 5, Fig. 1) as compared to sub-humid climate conditions, resulting in a significant decrease of  $K_{cb}$  and contributing most to the scatter in the relation between  $K_{cb}$  and  $LAI$  (Fig. 3). A further reduction of  $K_{cb}$  and additional contribution to the scatter were due to the higher stomatal control (Fig. 3), and in Vigevano and Domanínek, due to the lower wind speed (Table 5, Fig. 1).

#### 3.3. Rooting depth

Potential vertical root growth rate ( $14 \text{ mm day}^{-1}$ ) was estimated from sequential coring in Vigevano where the rooting depth increased from 0.45 m to 1.8 m between July 2004, and September 2004. The maximum rooting depth was determined to be about 2.0 m in Vigevano and about 1.5 m in Domanínek. In Lochristi, the dynamic maximum rooting depth determined by combination of soil coring and water table measurements (see Section 2.8) was estimated to reach 0.5 m in 2010 and to vary between 0.7 and 0.9 m afterwards.

#### 3.4. Model validation

##### 3.4.1. Validation by soil water content measurements

Reasonable agreement between measured and simulated  $SWC$  was found across all three sites with mean  $NSE$  values in the range of 0.59–0.85 (Table 6, Fig. 4). The systematic errors ( $ME$ ) were very small at all three sites, with a maximum of  $0.02 \text{ m}^3 \text{ m}^{-3}$  in Lochristi. Considering that in Vigevano only one sensor integrating the upper layer was used (Table 3), the agreement between measurements and simulations with a mean  $NSE$  of 0.59 and  $R^2$  of 0.65 was reasonable. In Domanínek, the occasional underestimates of  $SWC$  indicated an overestimation of some outflow or an inaccurate quantification of some inflow water balance components, or incorrect estimates of the soil water holding capacity. In contrast, the model sometimes overestimated  $SWC$  in Lochristi, indicating a potential underestimation of soil water loss, and consequently also of  $ET$ .

##### 3.4.2. Validation by micrometeorological methods

The average long-term energy balance closure was 0.82 (Vigevano), 0.91 (Domanínek  $EC_{OP}$ ), 0.95 (Domanínek  $EC_{EP}$ ) and 0.69 (Lochristi). In Vigevano, the simulated versus measured  $ET$  agreed best when  $H$  adj. of  $EC$  data was applied (Fig. 5 and Table 7a). In Domanínek, but

**Table 5**

Summary of mean annual weather conditions including air temperature ( $T_a$ ), minimum daily relative humidity ( $RH_{min}$ ), wind speed measured at 2 m above the ground ( $u_2$ ), daily sums of incoming short-wave radiation ( $R_G$ ), precipitation ( $P$ ) and reference evapotranspiration ( $ET_o$ ). The numbers in brackets represent the long-term (1961–1990) averages (Hijmans et al., 2005).

Site	Period	$T_a$ ( $^\circ\text{C}$ )	$RH_{min}$ (%)	$u_2$ ( $\text{m s}^{-1}$ )	$R_G$ ( $\text{MJ day}^{-1}$ )	$P$ (mm)	$ET_o$ (mm)
Vigevano (IT)	2004–2006	12.6 (12.7)	60	1.3	13.7	669 (998)	860 (803)
Domanínek (CZ)	2008–2015	7.6 (7)	68	1.7	10.5	609 (633)	617 (644)
Lochristi (BE)	2010–2013	10.6 (10.3)	62	2.4	10.2	912 (756)	666 (663)

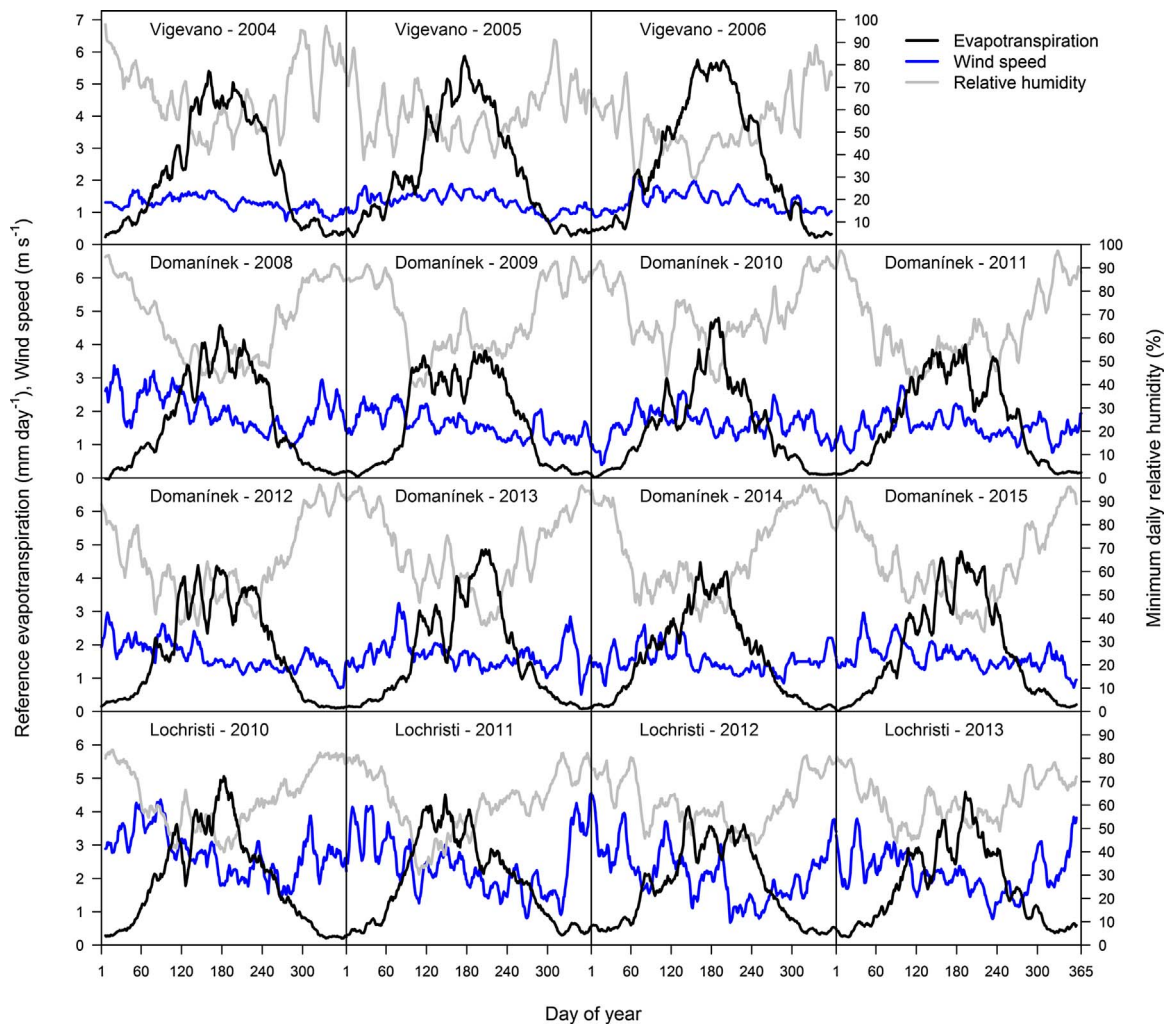


Fig. 1. Seasonal course (14-days rolling means) of the atmospheric evaporative demand expressed as reference evapotranspiration ( $ET_o$ ), daily minimum relative humidity ( $RH_{\min}$ ) and mean daily wind speed at 2 m above the ground ( $u_2$ ) at the three study sites during the selected years of observation. A high atmospheric evaporative demand is characterized by a high  $ET_o$ , high  $u_2$ , but low  $RH_{\min}$ .

especially in Lochristi, the  $ET$  simulations typically showed a better agreement (in terms of  $R^2$ ) with the measurements in the case of the Bowen adj. or the LE adj., as compared to the H adj. (Fig. 5, Tables 7b and 7c). In line with the average energy balance closure, the post-closure adjustment had the largest effect in the case of Lochristi (Table 7c).

In the case of Vigevano and Domanínek, the effect of post-closure adjustment resulted in a decrease of  $NSE$  and  $MBE$ , while  $R^2$  mostly remained the same (Tables 7a and 7b). The high energy balance closure at the Domanínek site generally resulted in very small differences between  $ET$  obtained from three post-closure scenarios. However, the sum of  $H$

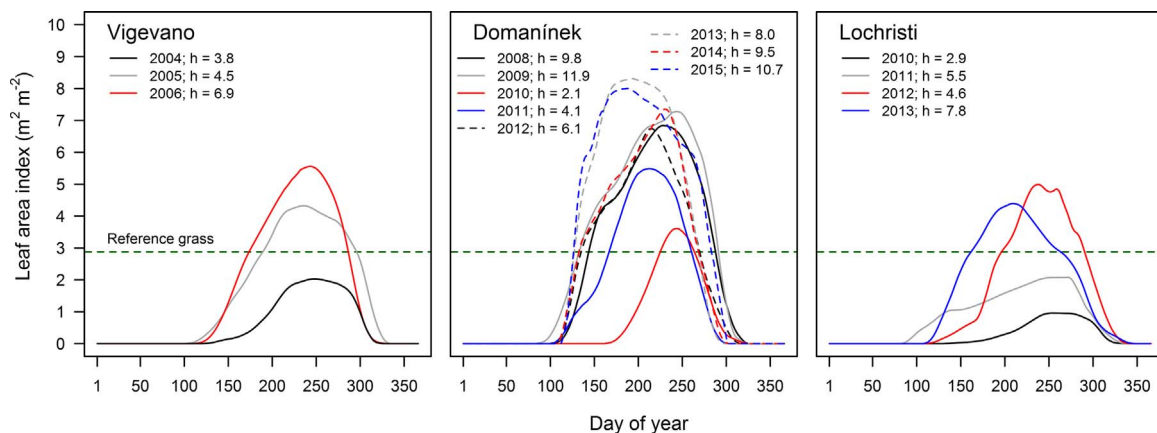
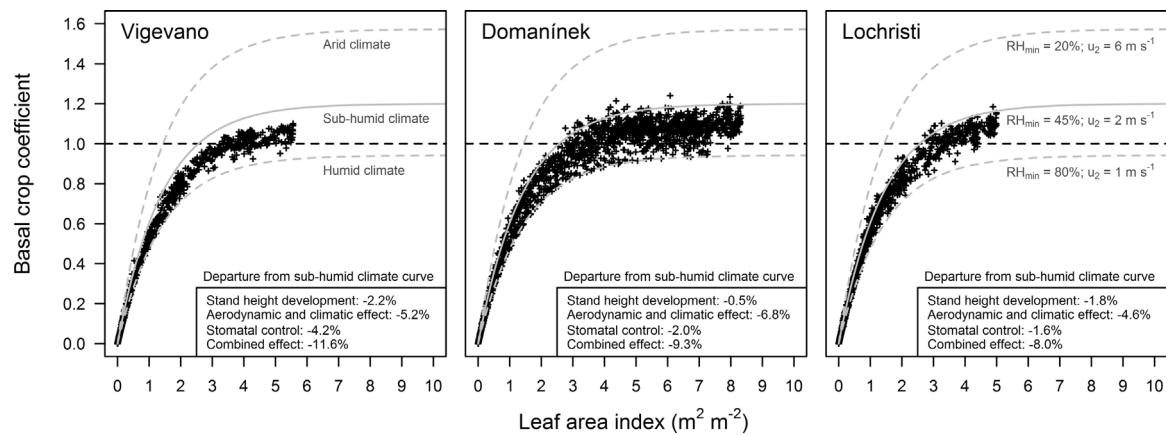


Fig. 2. Seasonal course of leaf area index (LAI) at the three investigated sites for the selected observation years. The measurements were interpolated using relationships with cumulative heat sum ( $> 5^\circ\text{C}$ ) and smoothed by a 14-day rolling mean. The horizontal green dashed line indicates the LAI (assumed to be constant) of the hypothetical reference grass cover. The end-of-season canopy height ( $h$ , m) is also provided.





**Fig. 3.** Relationship between simulated basal crop coefficient ( $K_{cb}$ ) and measured leaf area index ( $LAI$ ) at the three study sites. The grey solid line depicts the idealized relation for a stand taller than 2 m and for climatic conditions with a daily minimum relative humidity ( $RH_{min}$ ) of 45% and a mean daily wind speed at 2 m ( $u_2$ ) of  $2 \text{ m s}^{-1}$  (sub-humid conditions assumed as a standard for crop coefficients listed in FAO-56). The percentage departure from the sub-humid curve due to different factors is summarized. The dashed grey lines depict the upper and lower  $K_{cb}$  boundaries for arid/windy ( $RH_{min} = 20\%$ ,  $u_2 = 6 \text{ m s}^{-1}$ ) conditions and humid/calm conditions ( $RH_{min} = 80\%$ ,  $u_2 = 1 \text{ m s}^{-1}$ ), respectively, for completely anisohydric plants taller than 2 m. The horizontal black dashed line indicates the crop coefficient of the hypothetical reference grass cover (with the constant  $LAI$  of 2.9) irrespective of climatic conditions.

and  $LE$  was several times exceeding the available energy  $R_n - G$ , resulting in the highest  $ET$  following  $H$  adj. In fact,  $H$  was often negative shortly after noon. Although simulated  $ET$  in Domanínek was on average 20% smaller than  $EC_{OP}$  and  $EC_{EP}$  (Table 7b and Fig. 5), it was 6% larger than the BREB measurements (Table 7b and Fig. 6). In line with the model underestimation of the  $EC$  measurements in Domanínek (Fig. 5), the  $EC_{OP}$  showed systematically higher values as compared to BREB (Fig. 7). In contrast,  $EC_{EP}$  showed better agreement with the BREB method (Fig. 7). Correspondingly, there was a relatively high disagreement between  $EC_{OP}$  and  $EC_{EP}$  systems positioned closely together at the Domanínek SRWC (Fig. 7).

### 3.5. Inter-annual and intra-annual variation in evapotranspiration

Measured and modeled  $ET$  varied throughout the season in

correspondence to  $ET_o$  (compare Figs. 8 and 9 with Fig. 1). The measured and modeled  $ET$  were the most tightly related to  $ET_o$  when leaf area developed and transpiration became the dominant component (compare Figs. 8 and 9 with Figs. 1 and 2). In contrast, when soil evaporation was the dominant  $ET$  component, the relationship with  $ET_o$  primarily depended on the frequency of wetting events and related water content of the surface soil layer (Fig. 4). Soil evaporation was the highest during the establishment phase or during years immediately after harvest, when the soil was less shaded by the canopy. The highest  $ET$  values, close to  $8 \text{ mm day}^{-1}$ , occurred in summer when the evaporative demand was the highest, and when  $LAI$  was close to its seasonal maximum.  $ET$  was generally lower during the years after establishment or after harvest (Fig. 8). At all three sites, several periods of water stress (Fig. 9), i.e. periods when  $SWC$  in the root zone was below the stress threshold (Eq. (5)), were detected. In Vigevano, this occurred

**Table 6**

Summary of the error statistics of simulations of soil water content for the three study sites. Presented statistical variables include number of observations ( $n$ ), coefficient of determination ( $R^2$ ), mean error ( $ME$ ), root mean square error ( $RMSE$ ), and Nash–Sutcliffe model efficiency ( $NSE$ ).

Vigevano (IT)									
Period	2004–2006			2004		2005		2006	
$n$	655			165		288		202	
$R^2$	0.65			0.80		0.61		0.62	
$ME$	0.01			0.02		0.02		0.00	
$RMSE$	0.03			0.03		0.03		0.04	
$NSE$	0.59			0.71		0.46		0.62	
Domanínek (CZ)									
Period	2008–2015	2008	2009	2010	2011	2012	2013	2014	2015
$n$	2314	137	287	354	249	285	328	318	356
$R^2$	0.81	0.84	0.69	0.30	0.63	0.89	0.89	0.74	0.87
$ME$	0.01	−0.03	0.01	0.01	0.01	0.00	0.01	0.02	0.00
$RMSE$	0.02	0.03	0.02	0.02	0.02	0.02	0.02	0.02	0.02
$NSE$	0.72	−0.20	0.49	0.09	0.38	0.81	0.74	0.36	0.85
Lochristi (BE)									
Period	2010–2013		2010		2011		2012		2013
$n$	1089		132		352		352		253
$R^2$	0.91		0.76		0.92		0.79		0.93
$ME$	0.02		0.01		0.02		0.02		0.01
$RMSE$	0.03		0.02		0.03		0.03		0.02
$NSE$	0.84		0.50		0.85		0.62		0.88

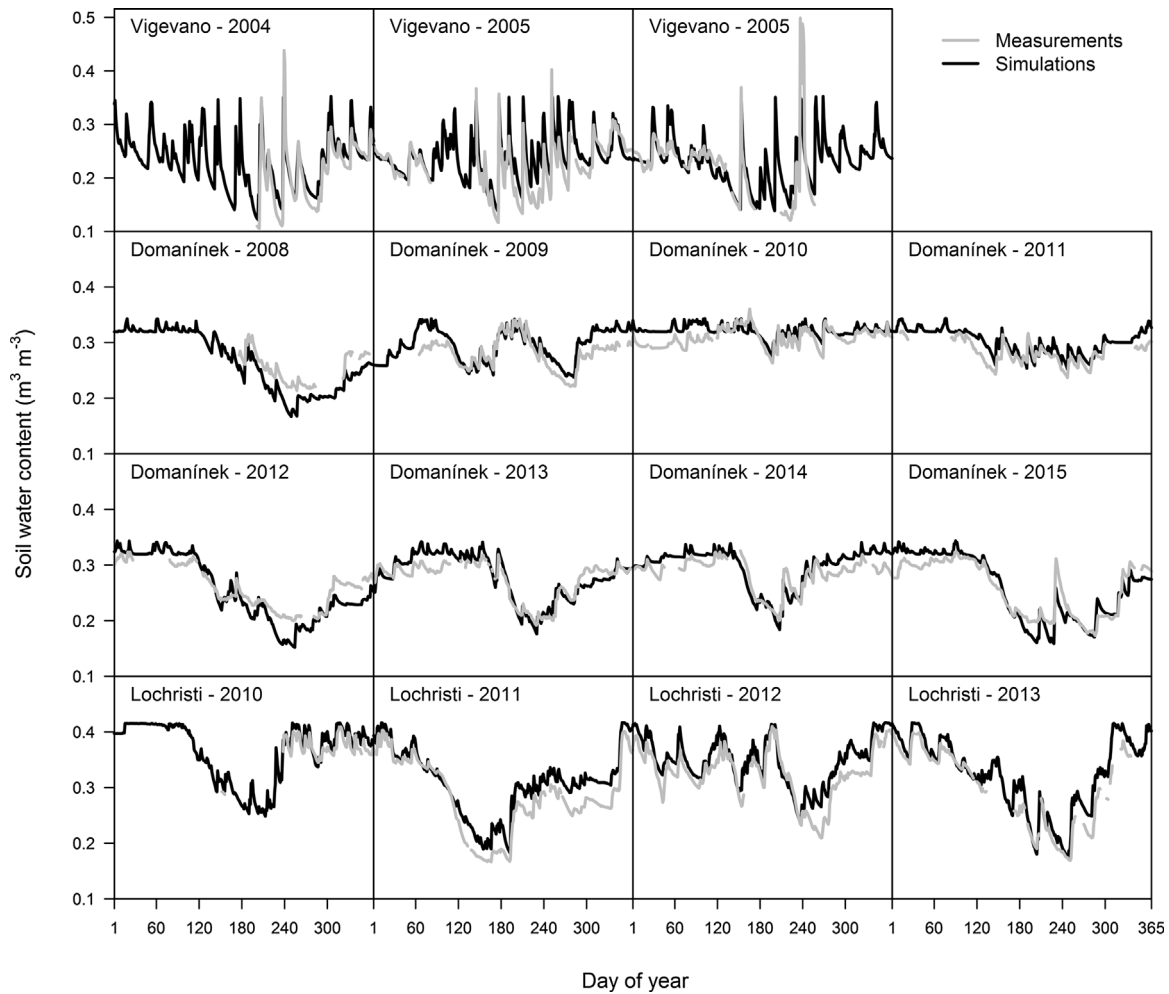


Fig. 4. Measured (grey) and simulated (black) values of soil water content for the three study sites for the selected years of observation. For Vigevano (IT) the line is representing a soil layer within 0–0.1 m. For Domanínek (CZ) the line represents an average from three soil depths – 0.1, 0.3 and 0.9 m. For Lochristi (BE) the presented data integrate the soil depths of 0.1, 0.2, 0.3, 0.4, 0.6, and 1.0 m.

only shortly during the establishment phase when root systems were not fully developed. This drought stress ended soon after irrigation. A limited water stress was also simulated between the second and third irrigation events in 2006. In Domanínek, the most pronounced ( $> 20\%$  transpiration reduction) water stress was simulated in the last year (2015) of the experiment. However, higher SWC and no transpiration reduction were identified by the measurements during that period. Thus, the model underestimated  $ET$ , as well as  $SWC$  during that period, suggesting additional soil water inflow than measured precipitation and simulated capillary rise. In Lochristi, the model correctly identified two short drought periods reported earlier (Broeckx et al., 2014; Zenone et al., 2015): the first during spring 2011, and the second, less intensive one, in summer 2013. Except of drought stress during the establishment phase in Vigevano, the remaining stress periods were characterized by a long-term (order of weeks to months) cumulative  $ET$  exceeding the cumulative precipitation and irrigation (Fig. 9).

### 3.6. Simulation of annual water balance components

The highest annual  $ET$  ( $751 \text{ mm y}^{-1}$ ) was simulated in Vigevano, while a comparable  $ET$  was simulated for Domanínek and Lochristi (Table 8). At none of the investigated sites did  $ET$  ever exceed  $ET_o$  on an annual time scale (Table 8, Fig. 9). Precipitation interception was on average 10% of  $ET$  across all three sites. Soil evaporation was the highest during years of planting or during years after harvest (70% of  $ET$  in 2010 at Lochristi). Soil evaporation was on average 26%, 14%

and 37% of  $ET$  in Vigevano, Domanínek and Lochristi, respectively. Deep percolation varied year by year depending mostly on precipitation and  $ET$  (Table 8). The high deep percolation losses, but also capillary rise rates, were typical for Lochristi due to the presence of a very shallow water table. On average, deep percolation in Lochristi represented 55% of precipitation and capillary rise. In contrast, the lowest deep percolation was simulated for Domanínek, averaging 25% of precipitation and capillary rise sum. As a consequence of the shallow water table in Lochristi, most of the transpiration uptake from the root zone was compensated by capillary rise. A smaller impact of capillary rise was found at the other two sites. Runoff was highest in Vigevano (11% of precipitation and irrigation sum), where basin irrigation was applied, and the lowest in Domanínek (1.5% of precipitation), characterized by the lowest precipitation.

Similar to  $LAI$ ,  $K_c$  generally increased with time after planting or harvest. The exception was the year 2012 in Lochristi, where during the year after harvest the highest annual  $K_c$  occurred. This was mainly due to the high annual precipitation and consequently the high soil evaporation, interception, and also transpiration. The mean annual  $K_c$  was 0.77, 0.88 and 0.82 in Vigevano, Domanínek and Lochristi, respectively. Since our sites did not exactly represent the sub-humid climate zone (Fig. 3), these  $K_c$  can be adjusted using a rearranged Eq. (2) (Allen et al., 1998). As a result, mean annual  $K_c$  would be 0.78, 0.91, 0.84 in Vigevano, Domanínek and Lochristi, respectively, if  $u_2 = 2 \text{ m s}^{-1}$  and  $RH_{\min} = 45\%$ . Considering this sub-humid climate zone correction during the years without any evident drought stress (Fig. 9), the mean

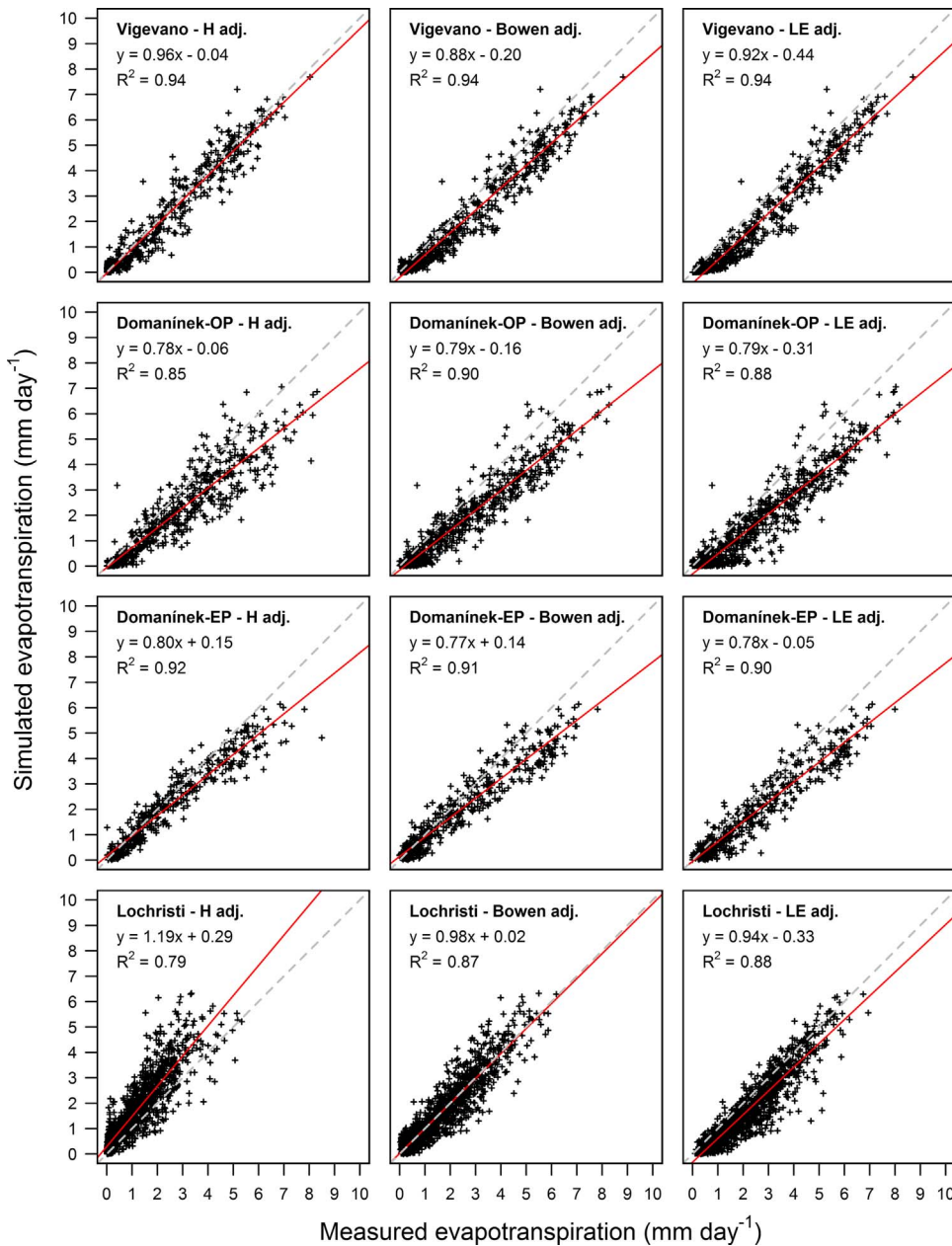


Fig. 5. Comparison of measured (by eddy covariance, EC) and model simulated daily evapotranspiration ( $ET$ ) for the three study sites. The EC measurements are represented for three energy balance closure scenarios: (i) the lack of energy balance closure is only due to sensible heat flux (H adj.) –  $ET$  of this scenario is identical to the measurement by EC; (ii) the lack of energy balance closure is distributed to both latent and sensible heat fluxes according to the Bowen ratio (Bowen adj.); (iii) the lack of energy balance closure is only due to the latent heat flux (LE adj.). At the Domanínek site, two comparisons are provided as  $ET$  was measured by open path (OP) and enclosed path (EP) EC systems. The solid line depicts the linear regression fit and the dashed line indicates the slope of unity.

annual  $K_c$  would be 0.85, 0.90 and 0.82 in Vigevano, Domanínek and Lochristi, respectively. This would result in an average  $K_c$  of 0.86 over all three sites under the above-mentioned criteria.

#### 4. Discussion

The model R-4ET based on the FAO-dual  $K_c$  approach (Allen, 2000; Kool et al., 2014) simulated  $ET$  of poplar SRWC reasonably well, however, there were several uncertainties linked not only to the model simulations, but also to the field measurements. In general, the field measurement uncertainties incorporate errors of all model inputs as well as the small-scale variability of observations – e.g.  $LAI$ ,  $SWC$  and rooting depth (Kersebaum et al., 2015). These initial errors can potentially be propagated through the model and increase in magnitude. Another main source of uncertainty is the model itself, inherently including simplifications and ignoring at least some water cycling mechanisms – e.g. underground water fluxes (Raes and Deproost, 2003; Sheikh et al., 2009). Nevertheless, when the model is compared with empirical data, discrepancies should not be exclusively ascribed to the

model, but a critical evaluation of all potential sources of error, including model inputs and validation data should be performed (Allen et al., 2011a,b).

Although EC is a direct micrometeorological method, often perceived as a standard technique for  $ET$  measurements (Allen et al., 2011a), there are difficulties of its use in testing models because of the lack of energy balance closure even after application of extensive corrections (Mauder and Foken, 2006), or proper quantification of all possible energy storage (Allen et al., 2011a; Foken, 2008; Foken et al., 2012). The most recent, yet heuristic, recommendation for model validation by EC data is to take into account three scenarios, H adj., Bowen adj. and LE adj., and treat them as a so called post-closure methods uncertainty band (Ingwersen et al., 2015). Experimental evidence of large-scale eddies transporting mainly heat suggests that the post-closure uncertainty band can be significantly narrowed towards H adj. scenario (Charuchittipan et al., 2014; Foken, 2008; Mauder and Foken, 2006). In our study, the simulated  $ET$  was typically within or close to the range between H adj. and Bowen adj. scenarios. While in Vigevano and Domanínek, H adj. provided generally better agreement

**Table 7a**

Summary of the error statistics of evapotranspiration simulations compared with three different eddy covariance (EC) post-closure scenarios for the Vigevano (IT) site. The energy balance closure residuum was either all assigned to sensible heat flux ( $EC_{H \text{ adj.}}$ ), was distributed to both sensible and latent heat flux according to the measured Bowen ratio ( $EC_{Bowen \text{ adj.}}$ ), or was all assigned to latent heat flux ( $EC_{LE \text{ adj.}}$ ). The provided statistical variables include number of observations ( $n$ ), coefficient of determination ( $R^2$ ), mean error ( $ME$ ), root mean square error ( $RMSE$ ), and Nash–Sutcliffe model efficiency ( $NSE$ ).

Vigevano				
$EC_{H \text{ adj.}}$				
Period	2004–2006	2004	2005	2006
$n$	506	131	267	108
$R^2$	0.94	0.89	0.95	0.96
$ME$	−0.12	−0.11	−0.19	0.04
$RMSE$	0.52	0.57	0.51	0.49
$NSE$	0.93	0.87	0.94	0.95
Vigevano				
$EC_{Bowen \text{ adj.}}$				
Period	2004–2006	2004	2005	2006
$n$	553	131	310	112
$R^2$	0.94	0.90	0.96	0.96
$ME$	−0.50	−0.56	−0.54	−0.32
$RMSE$	0.73	0.82	0.75	0.57
$NSE$	0.89	0.81	0.89	0.94
Vigevano				
$EC_{LE \text{ adj.}}$				
Period	2004–2006	2004	2005	2006
$n$	555	132	310	113
$R^2$	0.94	0.93	0.95	0.95
$ME$	−0.66	−0.65	−0.70	−0.54
$RMSE$	0.83	0.83	0.86	0.74
$NSE$	0.84	0.80	0.84	0.88

with model simulations, in Lochristi, the best agreement was achieved using Bowen adj.

The disagreement between EC with the BREB and the model in Domanínek can be explained in at least two different ways. Firstly, both EC and BREB could be affected either by measurements conducted too close to the canopy top (in attempt to minimize the short fetch impacts) making the fluxes less representative for the entire stand. Measurements in the roughness sublayer are compromised by the lack of flux spatial homogeneity (Katul et al., 1999) and could also contribute – beside the differences in type of analyzer and their frequency response correction requirements (Table 2) – to the systematic overestimation of  $EC_{OP}$  over  $EC_{EP}$ . Secondly, EC exceeding both the BREB method and the simulations might indicate that EC measurements were affected more by enhanced  $ET$  from the edges due to differences in footprints between the BREB and EC methods (Horst, 1999; Schmid, 2002; Stannard, 1997). Trees at the edges of the SRWC plantation likely transpired more due to their higher light interception, possibly higher water and nutrient uptake from outside the plantation, and due to a lower aerodynamic resistance and higher vapor pressure deficit (Cienciala et al., 2002). The model simulations as well as the SWC measurements represented the water balance in the interior zone. Thus, a better agreement between the model and the SWC measurements as compared to EC is not unexpected as the micrometeorological measurements might be contaminated by the contribution from edge zones.

Some differences between measurements and the model at the Domanínek site also emerged due to the short period when the model simulated water stress with partial stomatal closure and reduced transpiration, but field measurements showed higher SWC and no  $ET$  decline during that time. This suggests that the SRWC at the Domanínek site had either deeper root systems than measured, or was receiving a

lateral water inflow from upslope, or the capillary rise from water table was underestimated. Lateral water inflow from upslope was also identified at a neighboring grassland field in another modelling study (Hlavinka et al., 2011), and it generally indicates the inability to properly simulate the water balance of complex terrain using a one-dimensional modelling approach (Sheikh et al., 2009). The overall discrepancy between the micrometeorological methods gives an idea of the uncertainty of  $ET$  measurements at the Domanínek plantation and will warrant further investigation. The size of the Domanínek plantation represents the scale of SRWC plantations in this region, which underscores the inherent challenges to correctly measure EC fluxes at SRWC plantations. Therefore, a combination of several methods as sap flow or leaf level gas exchange measurements coupled with modelling is recommended for further investigation at stands of similar size.

The sum of turbulent energy fluxes occasionally exceeding available energy indicates an additional source of energy due to advection of  $H$ , supporting the edge effect concern in Domanínek. Similar results with  $ET$  exceeding the available energy and frequent negative  $H$  has been reported for plantations with similar dimensions as at the Domanínek (Allen et al., 1999; Hall et al., 1998; Lindroth and Iritz, 1993) and in a phytoremediation study with unspecified number of trees around the edges of the lysimeters (Guidi et al., 2008). A certain amount of advection can be realistic, even at very large scale in arid and semi-arid climates. The potential  $K_c$  under such conditions can be inferred from the presented arid climate curve (Fig. 3). Under arid climatic conditions, characterized by high  $T_a$  and low  $RH_{min}$ , a potential enhancement of  $ET$  is more pronounced for taller, better ventilated canopies and thus increases with wind speed (Allen et al., 2011a). This mechanism might be a potential explanation for very high  $K_{cb}$  ( $\sim 1.8$ ) reported from south-west England during one hot and exceptionally dry summer (Hall



**Table 7b**

Summary of the error statistics of evapotranspiration simulations compared with Bowen ratio energy balance (BREB) measurements and with three different eddy covariance (EC) post-closure scenarios for the Domanínek (CZ) site. Eddy covariance measurements were performed with either open path (EC<sub>OP</sub>), or enclosed path (EC<sub>EP</sub>) infrared gas analyzer. The energy balance closure residuum was either all assigned to sensible heat flux (EC<sub>H</sub> adj.), was distributed to both sensible and latent heat flux according to the measured Bowen ratio (EC<sub>Bowen</sub> adj.), or was all assigned to latent heat flux (EC<sub>LE</sub> adj.). The provided statistical variables include number of observations (*n*), coefficient of determination (*R*<sup>2</sup>), mean error (*ME*), root mean square error (*RMSE*), and Nash–Sutcliffe model efficiency (*NSE*).

Domanínek									
BREB									
Period	2008–2015	2008	2009	2010	2011	2012	2013	2014	2015
$n$	1735	146	237	216	255	253	130	257	241
$R^2$	0.87	0.89	0.90	0.85	0.95	0.86	0.81	0.90	0.92
$ME$	0.08	0.58	0.04	0.11	0.05	0.22	0.47	−0.22	−0.25
$RMSE$	0.62	0.84	0.57	0.47	0.38	0.69	0.99	0.53	0.56
$NSE$	0.83	0.60	0.85	0.79	0.94	0.80	0.47	0.86	0.89
EC <sub>OP</sub> H adj.									
Period	2011–2014	2011	2012	2013	2014	2015			
$n$	575	110	143	150	172	575			
$R^2$	0.85	0.91	0.89	0.85	0.88	0.85			
$ME$	−0.64	−0.27	−0.34	−0.61	−1.15	−0.64			
$RMSE$	1.01	0.56	0.76	0.93	1.40	1.01			
$NSE$	0.74	0.87	0.87	0.70	0.52	0.74			
EC <sub>OP</sub> Bowen adj.									
$n$	627	117	147	182	181	627			
$R^2$	0.90	0.94	0.91	0.75	0.92	0.90			
$ME$	−0.72	−1.09	−0.61	−0.54	−0.76	−0.72			
$RMSE$	0.99	1.23	0.92	0.86	1.00	0.99			
$NSE$	0.76	0.61	0.82	0.60	0.74	0.76			
EC <sub>OP</sub> LE adj.									
$n$	657	121	155	193	188	657			
$R^2$	0.88	0.91	0.9	0.69	0.92	0.88			
$ME$	−0.88	−1.26	−0.81	−0.78	−0.79	−0.88			
$RMSE$	1.13	1.41	1.07	1.09	1.00	1.13			
$NSE$	0.67	0.48	0.75	0.36	0.73	0.67			
EC <sub>EP</sub> H adj.									
Period	2013–2015	2013	2014	2015					
$n$	387	20	166	201					
$R^2$	0.92	0.78	0.93	0.90					
$ME$	−0.35	−0.29	−0.29	−0.41					
$RMSE$	0.70	0.37	0.64	0.76					
$NSE$	0.87	0.39	0.89	0.84					
EC <sub>EP</sub> Bowen adj.									
$n$	436	25	180	231					
$R^2$	0.91	0.75	0.94	0.89					
$ME$	−0.41	−0.29	−0.45	−0.39					
$RMSE$	0.78	0.39	0.78	0.81					
$NSE$	0.85	0.45	0.86	0.83					
EC <sub>EP</sub> LE adj.									
$n$	434	26	180	228					
$R^2$	0.90	0.74	0.94	0.87					
$ME$	−0.61	−0.48	−0.67	−0.58					
$RMSE$	0.90	0.56	0.91	0.92					
$NSE$	0.79	0.09	0.80	0.77					

et al., 1996, 1998) for poplar clones with weak stomatal control (Allen et al., 1999). However, the aridity itself cannot explain exceedingly high *K<sub>c</sub>* of 4.0–5.0 reported from a lysimetric study in Italy (Guidi et al., 2008). Such *K<sub>c</sub>* would not be realistic at larger scales where the advection of sensible heat is dampening the turbulence and therefore the exchange of scalars, including *ET* and the advection itself (Allen et al., 2011a). Note that neither the *K<sub>c</sub>* presented in Hall et al. (1998) nor the one described in Guidi et al. (2008) were adjusted for climate (Eq. (2)) and therefore are not compatible with the FAO-56 list.

The average fraction of *ET* represented by soil evaporation in this study (22%) agreed well with 23% for willow SRWC from Sweden (Iritz et al., 2001; Persson and Lindroth, 1994), and with 25% for poplar SRWC from northeast Germany (Bungart and Hüttl, 2004). Rather low soil evaporation fraction in Domanínek (14%) was caused by the high *LAI* limiting the below canopy available energy and due to high mulch effect provided by the decomposing litter. The parameters characterizing the rate of litter decomposition were adopted from the literature

(Odhambo and Irmak, 2012) and require further testing and an eventual refinement which can potentially affect soil evaporation simulations. Interception, representing on average 8% of precipitation and 10% of *ET* across all three sites, fell well into the range in literature (Bungart and Hüttl, 2004; Hall et al., 1996; Persson and Lindroth, 1994) and agreed with our measurements at other plantations (Fischer et al., 2013a). Interception can be an additional source of disagreement between modeled and measured *ET* due to the inherent challenges to measure *ET* during conditions when rain interception is occurring (van Dijk et al., 2015).

The average fraction of *ET* represented by transpiration (66%) was in close agreement with other studies (Bungart and Hüttl, 2004; Fischer et al., 2013a; Iritz et al., 2001; Persson and Lindroth, 1994). As an independent test of *ET* partitioning, we calculated water use efficiency (*WUE*, g kg<sup>−1</sup>) using the available AWB productivity data. The *WUE* based on inventory data and simulated *ET* yielded values of 1.9, 2.0 and 1.5 g kg<sup>−1</sup> for Vigeveno, Domanínek, and Lochristi, respectively. More

**Table 7c**

Summary of error statistics of evapotranspiration simulations compared with three different eddy covariance post-closure scenarios for the Lochristi (BE) site. The energy balance closure residuum was either all assigned to sensible heat flux ( $EC_{H \text{ adj.}}$ ), was distributed to both sensible and latent heat fluxes according to the measured Bowen ratio ( $EC_{Bowen \text{ adj.}}$ ), or was all assigned to latent heat flux ( $EC_{LE \text{ adj.}}$ ). The provided statistical variables include number of observations ( $n$ ), coefficient of determination ( $R^2$ ), mean error ( $ME$ ), root mean square error ( $RMSE$ ), and Nash–Sutcliffe model efficiency ( $NSE$ ).

Lochristi					
Period	2010–2013	2010	2011	2012	2013
$EC_{H \text{ adj.}}$					
$n$	1226	192	355	340	339
$R^2$	0.79	0.78	0.82	0.87	0.74
$ME$	0.49	0.30	0.56	0.46	0.56
$RMSE$	0.81	0.62	0.80	0.72	0.99
$NSE$	0.36	0.55	0.03	0.59	0.24
$EC_{Bowen \text{ adj.}}$					
$n$	1244	196	357	343	348
$R^2$	0.87	0.81	0.84	0.91	0.89
$ME$	0.00	−0.17	0.04	0.04	0.00
$RMSE$	0.49	0.53	0.48	0.44	0.52
$NSE$	0.86	0.77	0.81	0.89	0.88
$EC_{LE \text{ adj.}}$					
$n$	1240	197	354	346	343
$R^2$	0.88	0.71	0.88	0.89	0.92
$ME$	−0.45	−0.52	−0.47	−0.37	−0.48
$RMSE$	0.66	0.84	0.63	0.60	0.65
$NSE$	0.76	0.53	0.73	0.80	0.83

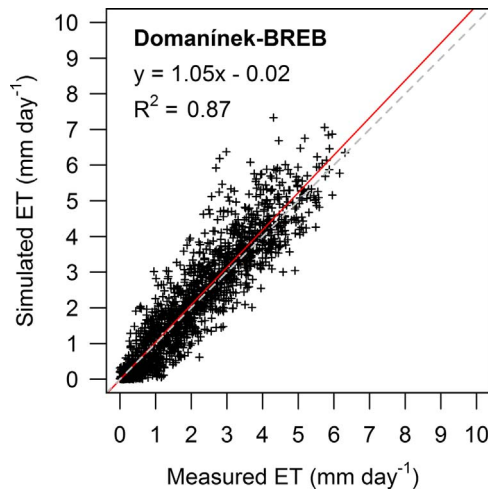


**Fig. 6.** Comparison of measured and simulated daily evapotranspiration ( $ET$ ) at the Domanínek (CZ) site. The solid line depicts the linear regression fit and the dashed line indicates the slope of unity.

Note that for the Bowen ratio energy balance (BREB) method, no scenarios are applied since the method closed the energy budget by definition.

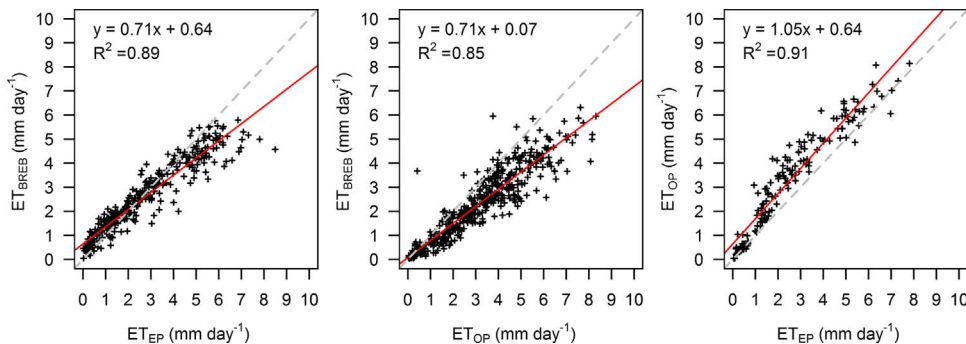


**Fig. 7.** Comparison of evapotranspiration ( $ET$ ) measured by different micrometeorological methods and instrumental setups at the Domanínek (CZ) site. The methods include Bowen ratio energy balance (BREB), open path (OP) eddy covariance, and enclosed path (EP) eddy covariance. The solid line depicts the linear regression fit and the dashed line indicates the slope of unity. No post-closure adjustment on eddy covariance fluxes was carried out in this comparison.

importantly, the  $WUE$  derived from simulated transpiration was 2.7, 2.8 and  $2.8 \text{ g kg}^{-1}$  for Vigevano, Domanínek, and Lochristi, respectively. These values are well within the range of  $1.8\text{--}3.3 \text{ g kg}^{-1}$  for poplar SRWC (reviewed by Fischer et al., 2015 and King et al., 2013). Moreover, the very high convergence of the transpiration based  $WUE$  originating from all three sites provided additional confidence in the  $ET$  partitioning and supported the robustness and general validity of our results.

Although the FAO-56 methodology is not primarily intended to simulate SWC (but rather  $ET$ ) due to several simplifications related to soil water movement (Allen et al., 1998; Raes et al., 2009; Steduto et al., 2009), the comparison with measurements can still indicate systematic simulation biases, since the model is based on the mass conservation law. In order to properly specify the soil volume involved in the water balance computations, special care is required in determining the rooting depth. While the rooting depth was set to consistently increase until it reached its maximum value in Vigevano and Domanínek, it was assumed to be dynamically varying due to the water table fluctuations in Lochristi. Despite the several assumptions adopted to simulate the water table driven temporal variation in rooting depth, the estimates were in good agreement with occasional *in situ* observations (Berhongaray et al., 2015; Berhongaray et al., 2017). Although deep percolation, runoff, and capillary rise were difficult to validate, as no relevant measurements were available, reliable estimates of SWC and  $ET$  supported the assumption that these terms were reasonably well simulated. In general, our estimates of deep percolation fell well within simulations for SRWC reported elsewhere (Bungart and Hüttl, 2004; Hall et al., 1996; Lasch et al., 2009). High deep percolation and runoff losses in Vigevano indicated that irrigation was not effectively distributed through time, whereas high deep percolation rates in Lochristi were the result of the high water table replenishing the root zone by capillary rise or by the water table presence in the root zone, as well as the result of the high precipitation inputs. Our comparison of the field measurements and model simulations at all the three sites suggests that precipitation records should preferably be adjusted to compensate for underestimation due to wind effects (Yang et al., 1998), otherwise less water would enter the system resulting in a higher calculated soil water depletion and reduced  $ET$ , which was not confirmed by SWC and  $ET$  observations in the current study. The need for adjustment of the precipitation records due to general rain-gauge underestimation was in agreement with several other water balance studies (Allen et al., 2011a; Fischer et al., 2013a; Persson and Lindroth, 1994).

The predicting ability of R-4ET was found satisfactory with error statistics comparable to other water balance studies calibrating models against measurements (Hlavinka et al., 2011; Horemans et al., 2017; Persson and Lindroth, 1994). The model R-4ET might be useful for the assessment of water use, evaluation of drought risk, or for eventual consideration of irrigation at sites where the establishment of SRWC plantations is being considered. Although the presented form of model R-4ET was developed and tested on SRWC, it might also be applied to other (bioenergy) crops because of the general principles involved. When using model simulations for future commercial SRWC

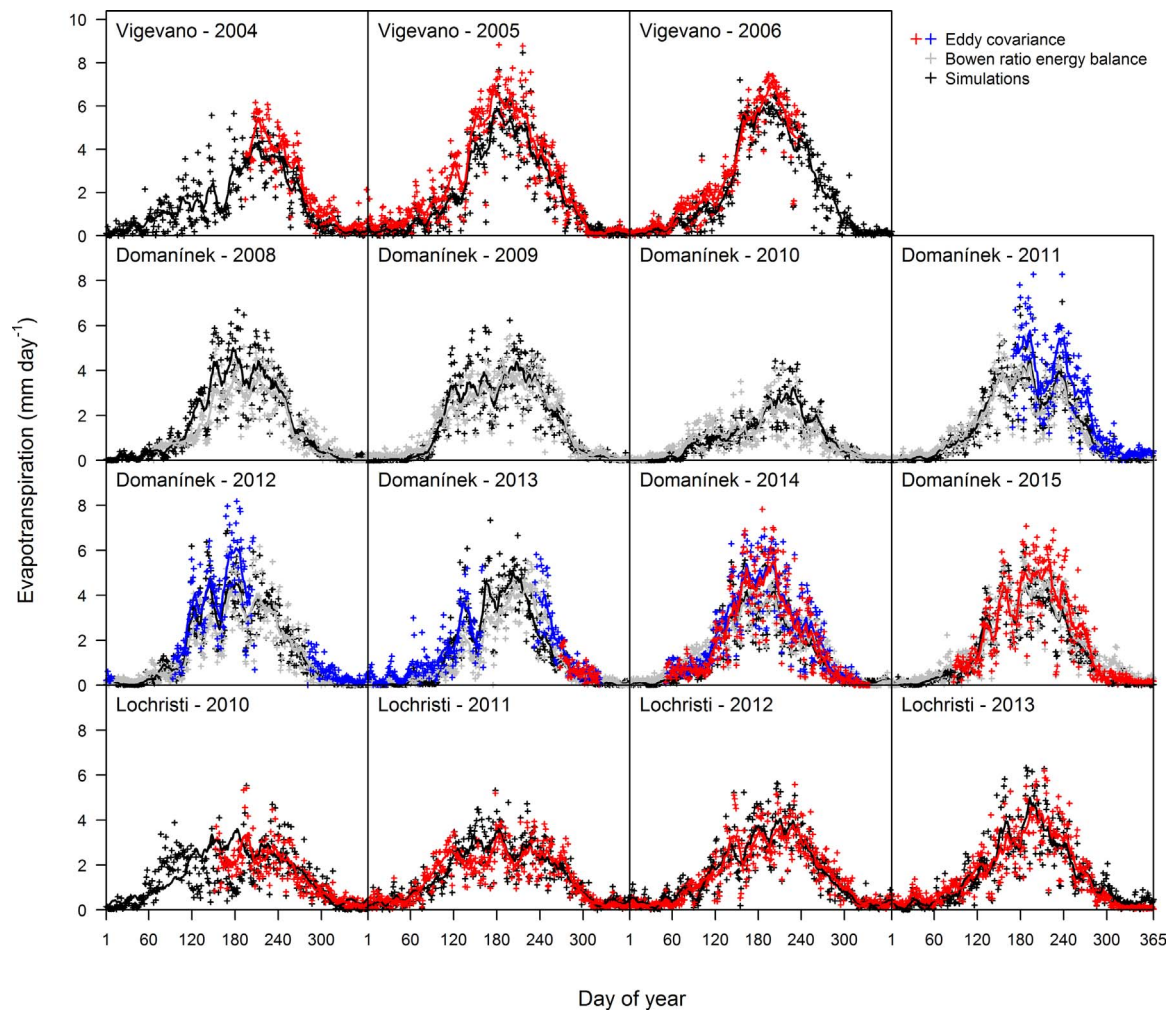


**Fig. 8.** Time series of simulated (black) and measured (red, blue and grey) evapotranspiration at the three study sites. All measurements were gap filled and eddy covariance (EC) data were Bowen-ratio adjusted. The EC measurements at the Domanínek (CZ) site were carried out either by open-path (blue) or enclosed-path (red) gas analyzers. The points represent individual daily totals and the lines show their 14-day rolling means.

plantations, the potential  $LAI$  should be considered (e.g. inferred from Fig. 2) as the required high productivity of SRWC is tightly linked with high  $LAI$  (Zenone et al., 2015). The model can be further used for regional SRWC water balance scaling (Hall et al., 1996; Lasch et al., 2009; Lindroth and Båth, 1999) since only a simple parameterization is needed, based on widely available soil data. Mechanistic models (Deckmyn et al., 2004, 2008; Ogée et al., 2003), with detailed, vertically stratified processes, could potentially provide a better agreement with experimental data and provide a better insight into particular processes. However, the primary intention of the present study was to keep parametrization simple and compatible with data availability at the farm level for further upscaling. In special cases when only a simple assessment is needed and seasonal variation of  $K_c$  can be ignored, use of an annual  $K_c$  of 0.86 representing an average value across the three sites in years with no evident drought stress seems reasonable. This  $K_c$  fits well within mean range of 0.8–0.9 based on an extensive literature review (Fischer et al., 2013b). It should be noted that the mean  $K_c$  of 0.86 was obtained from plantations with productivity close to a reported average of 8–10  $Mg\ ha^{-1}\ y^{-1}$  for poplar and willow SRWC (King et al., 2013), making this  $K_c$  value representative. Although the variability of  $K_c$  with genotype and site is expectable,  $K_c$  which significantly deviates from those provided in our study and those resulting from FAO-56 methodology (Allen et al., 1998) should be critically evaluated for all potential sources of errors (Allen et al., 2011a).

The FAO-56 approach generally works well for crops with low

stomatal control and anisohydric hydraulic strategy (Allen et al., 1998). In our approach, we considered the increase of stomatal resistance with increasing vapor pressure deficit (Novick et al., 2016; Oren et al., 1999), but further testing is necessary as hydraulic strategy may vary throughout the season and with genotype (Bloemen et al., 2017; Oren et al., 1999; Schmidt-Walter et al., 2014). Finally, the results of this comparative study can neither support nor contradict the previous concerns about SWRC water use on the hydrology of agricultural landscapes (Hall et al., 1996, 1998). Rather, they provide a quantitative assessment tool. Concerns about the water use by SRWC should be based on realistic assumptions about the potential land-use change (Zenone et al., 2016), as they otherwise result in unjustified decisions and have a negative effect on the development of a sustainable energy industry.

## 5. Conclusions

Measurement and modelling at the three sites across Europe covering in total 15 years of data demonstrated that  $ET$  of SRWC is generally lower than  $ET_0$  and  $ET$  of highly productive crops at an annual time scale (mean  $K_c$  of 0.86) while it can be similar or slightly higher at daily to monthly time scales (maximum  $K_c$  of 1.20). The  $ET$  and  $K_c$  values obtained in our study were significantly lower than the former reports that have raised concerns from extensive SRWC plantations with excessively high water use. Crop coefficients which significantly

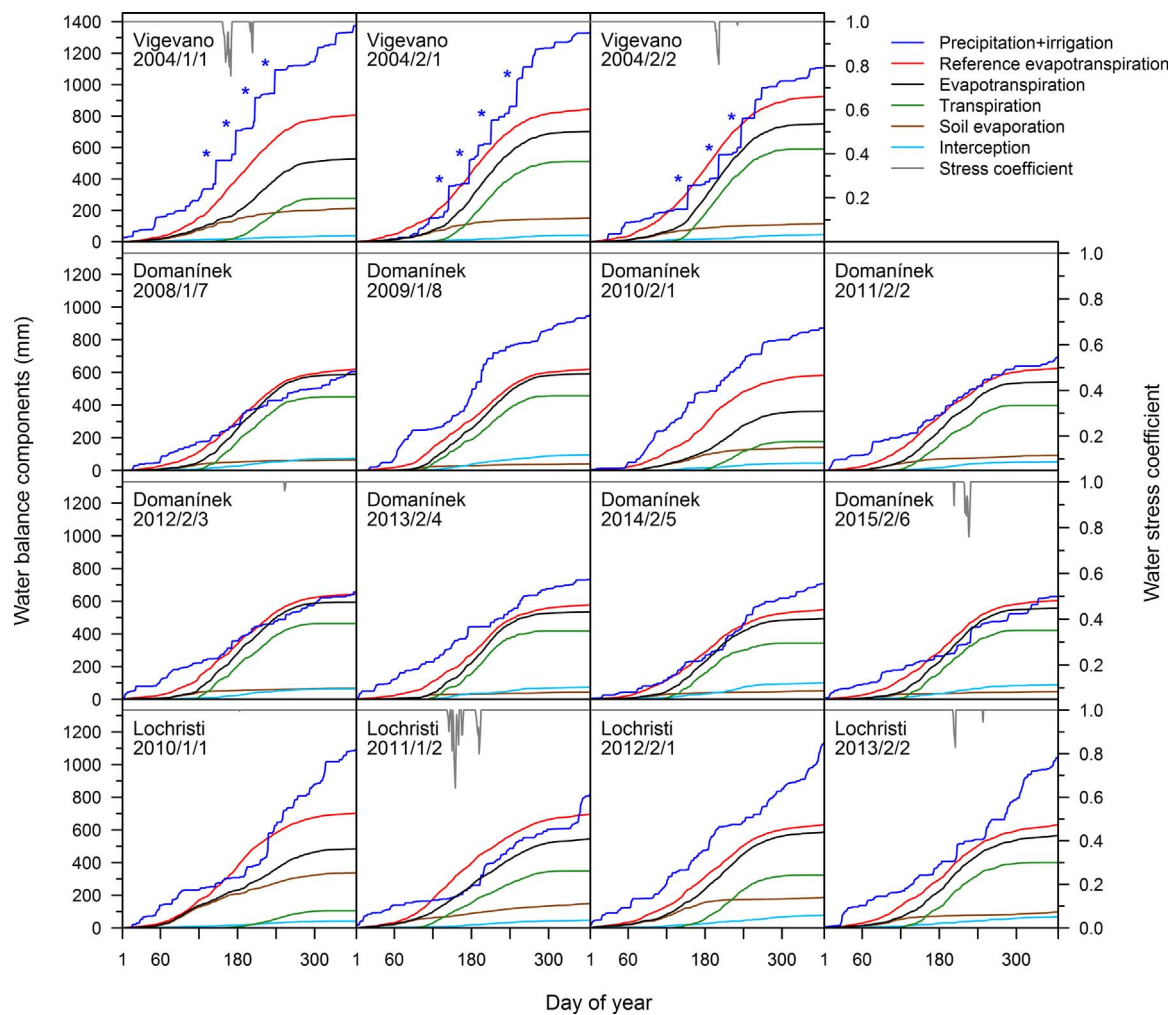


Fig. 9. Simulated cumulative annual water balance components for the three investigated sites and years of the observation. The soil water stress coefficient is also provided. The numerical codes indicate year/rotation/year within the rotation. The blue stars indicate the irrigation (applied only in Vigevano, IT).

differ from those provided in our study or those resulting from FAO-56 methodology (e.g.  $ET$  exceeding available energy water equivalent) should first be critically evaluated for all potential sources of errors, including lack of fetch, oasis effect, or scaling issues, and

representativeness of such results carefully evaluated. Our results suggested that the model R-4ET, based on the FAO-dual  $K_c$  approach (originally designed for crops), can provide reasonable estimates of the water use and the water balance of a poplar SRWC. The resulting

Table 8

Simulated annual water balance components (mm) and crop coefficients for the three study sites and for all the years of the observations.

Year	Precipitation (Irrigation)	Reference evapotranspiration	Evapotranspiration	Crop coefficient	Soil evaporation	Interception	Transpiration	Capillary rise	Deep percolation	Runoff
Vigevano (IT)										
2004	774 (600)	808	528	0.65	213	38	277	9	695	173
2005	728 (600)	845	702	0.83	151	41	511	13	506	144
2006	659 (450)	926	751	0.81	115	46	590	22	284	95
Domanínek (CZ)										
2008	606	621	588	0.95	65	74	450	28	129	1
2009	960	620	591	0.95	40	94	457	26	249	50
2010	871	583	362	0.62	141	44	176	18	519	22
2011	694	625	541	0.87	92	53	397	40	177	7
2012	656	643	594	0.92	68	63	463	36	184	5
2013	732	578	534	0.92	44	73	418	29	148	9
2014	706	548	494	0.90	51	100	343	17	210	8
2015	629	604	557	0.92	47	88	422	30	148	11
Lochristi (BE)										
2010	1090	702	483	0.69	337	41	105	301	810	99
2011	817	696	545	0.78	149	47	348	327	560	25
2012	1136	633	587	0.93	187	77	323	316	764	24
2013	1043	631	566	0.90	98	68	400	279	802	29



annual  $K_c$  values from the years without drought stress, but mainly the model itself, can be used for upscaling the poplar SWRC water balance since they were found to be robust across three different sites.

## Notice of copyright

This manuscript has been authored by UT-Battelle, LLC under Contract No. DE-AC05-00OR22725 with the U.S. Department of Energy. The United States Government retains and the publisher, by accepting the article for publication, acknowledges that the United States Government retains a non-exclusive, paid-up, irrevocable, worldwide license to publish or reproduce the published form of this manuscript, or allow others to do so, for United States Government purposes. The Department of Energy will provide public access to these results of federally sponsored research in accordance with the DOE Public Access Plan (<http://energy.gov/downloads/doe-public-access-plan>).

## Acknowledgements

The research leading to these results was supported by the Czech Ministry of Education, Youth and Sports of CR within the National Sustainability Program I (NPU I) as grant # LO1415 as well as by the European Commission's Seventh Framework Program (FP7/2007–2013) through the European Research Council as ERC grant agreement # 233366 (POPFULL) and through the People Program/Marie Curie Actions as REA grant agreement # PIIF-GA-2013-624245 (SRF-OZO). This material is based upon work supported by the U.S. Department of Energy, Office of Science, Office of Biological and Environmental Research under contract # DE-AC05-00OR22725.

## References

- Allen, R.G., Pereira, L.S., Raes, D. and Smith, M., 1998. Crop evapotranspiration – Guidelines for computing crop water requirements – FAO Irrigation and drainage paper 56, Rome, Italy, 290 pp.
- Allen, S.J., Hall, R.L., Rosier, P.T., 1999. Transpiration by two poplar varieties grown as coppice for biomass production. *Tree Physiol.* 19, 493–501.
- Allen, R.G., Pereira, L.S., Howell, T.A., Jensen, M.E., 2011a. Evapotranspiration information reporting: I: Factors governing measurement accuracy. *Agric. Water Manage.* 98, 899–920.
- Allen, R.G., Pereira, L.S., Howell, T.A., Jensen, M.E., 2011b. Evapotranspiration information reporting: II: recommended documentation. *Agric. Water Manage.* 98, 921–929.
- Allen, R.G., 2000. Using the FAO-56 dual crop coefficient method over an irrigated region as part of an evapotranspiration intercomparison study. *J. Hydrol.* 229, 27–41.
- Anderson, H.W., Papadopol, C.S., Zsuffa, L., 1983. Wood energy plantations in temperate climates. *For. Ecol. Manage.* 6, 281–306.
- Berhongaray, G., King, J.S., Janssens, I.A., Ceulemans, R., 2012. An optimized fine root sampling methodology balancing accuracy and time investment. *Plant Soil* 366, 351–361.
- Berhongaray, G., Janssens, I.A., King, J.S., Ceulemans, R., 2013. Fine root biomass and turnover of two fast-growing poplar genotypes in a short-rotation coppice culture. *Plant Soil* 373, 269–283.
- Berhongaray, G., Verlinden, M.S., Broeckx, L.S., Ceulemans, R., 2015. Changes in belowground biomass after coppice in two *Populus* genotypes. *For. Ecol. Manage.* 337 (Suppl. C), 1–10.
- Berhongaray, G., Verlinden, M.S., Broeckx, L.S., Janssens, I.A., Ceulemans, R., 2017. Soil carbon and belowground carbon balance of a short-rotation coppice: assessments from three different approaches. *Glob. Change Biol. Bioenergy* 9, 299–313.
- Bloemen, J., et al., 2017. Water use of a multi-genotype poplar short-rotation coppice from tree to stand scale. *Glob. Change Biol. Bioenergy* 9, 370–384.
- Brisson, N., et al., 2003. An overview of the crop model STICS. *Eur. J. Agron.* 18, 309–332.
- Broadfoot, W.M., 1973. Water table depth and growth of young cottonwood. Research Note SO-RN-167, USDA-Forest Service, Southern Forest Experiment Station, New Orleans, LA, 4 pp.
- Broeckx, L.S., Verlinden, M.S., Ceulemans, R., 2012. Establishment and two-year growth of a bio-energy plantation with fast-growing *Populus* trees in Flanders (Belgium): Effects of genotype and former land use. *Biomass Bioenergy* 42, 151–163.
- Broeckx, L.S., et al., 2014. The effect of a dry spring on seasonal carbon allocation and vegetation dynamics in a poplar bioenergy plantation. *Glob. Change Biol. Bioenergy* 6, 473–487.
- Broeckx, L., Vanbever, S., Verlinden, M., Ceulemans, R., 2015. First vs. second rotation of a poplar short rotation coppice: leaf area development, light interception and radiation use efficiency. *iForest – Biogeosci. For.* 8, 565–573.
- Bungart, R., Hüttl, R.F., 2004. Growth dynamics and biomass accumulation of 8-year-old hybrid poplar clones in a short-rotation plantation on a clayey-sandy mining substrate with respect to plant nutrition and water budget. *Eur. J. For. Res.* 123, 105–115.
- Campbell, G.S., 1986. Extinction coefficients for radiation in plant canopies calculated using an ellipsoidal inclination angle distribution. *Agric. For. Meteorol.* 36, 317–321.
- Charuchittiparn, D., Babel, W., Mauder, M., Leps, J.P., Foken, T., 2014. Extension of the averaging time in eddy-covariance measurements and its effect on the energy balance closure. *Boundary-Layer Meteorol.* 152, 303–327.
- Cienciala, E., et al., 2002. The effect of a north-facing forest edge on tree water use in a boreal Scots pine stand. *Can. J. For. Res.* 32, 693–702.
- Deckmyn, G., Laureysens, I., Garcia, J., Muys, B., Ceulemans, R., 2004. Poplar growth and yield in short rotation coppice: model simulations using the process model SECRETS. *Biomass Bioenergy* 26, 221–227.
- Deckmyn, G., et al., 2008. ANAFORE: A stand-scale process-based forest model that includes wood tissue development and labile carbon storage in trees. *Ecol. Modell.* 215, 345–368.
- Dickmann, D.I., Isebrands, J.G., Blake, T.J., Kosola, K., Kort, J., 2001. Physiological ecology of poplars. In: Dickmann, D.I., Isebrands, J.G., Eckenwalder, J.E., Richardson, J. (Eds.), *Poplar Culture in North America*. NRC Research Press, Ottawa, Canada, pp. 77–118.
- Djomo, S.N., Kasmoui, O.E., Ceulemans, R., 2011. Energy and greenhouse gas balance of bioenergy production from poplar and willow: a review. *Glob. Change Biol. Bioenergy* 3, 181–197.
- Droogers, P., Allen, R.G., 2002. Estimating reference evapotranspiration under inaccurate data conditions. *Irrig. Drain. Syst.* 16, 33–45.
- Falge, E., et al., 2001. Gap filling strategies for long term energy flux data sets. *Agric. For. Meteorol.* 107, 71–77.
- Falge, E., et al., 2005. Comparison of surface energy exchange models with eddy flux data in forest and grassland ecosystems of Germany. *Ecol. Modell.* 188, 174–216.
- Fischer, M., et al., 2013a. Annual and intra-annual water balance components of a short rotation poplar coppice based on sap flow and micrometeorological and hydrological approaches. *International Society for Horticultural Science (ISHS)*, Leuven, Belgium, pp. 401–408.
- Fischer, M., et al., 2013b. Evapotranspiration of a high-density poplar stand in comparison with a reference grass cover in the Czech–Moravian Highlands. *Agric. Forest Meteorol.* 181, 43–60.
- Fischer, M., et al., 2015. *Populus* and *Salix* grown in a short-rotation coppice for bioenergy: ecophysiology, aboveground productivity, and stand-level water use efficiency. In: Bhardwaj Ajay, K., Zenone, T., Chen, J. (Eds.), *Sustainable Biofuels, An Ecological Assessment of the Future Energy*. HEP deGruyter, Berlin-Beijing, pp. 157–194.
- Fischer, M., et al., 2017. A critical analysis of species selection and high vs. low-input silviculture on establishment success and early productivity of model short-rotation wood-energy cropping systems. *Biomass Bioenergy* 98, 214–227.
- Fischer, M. et al., 2018. Development and testing of poplar short rotation coppice water balance model R-4ET. *Agricultural Water Management*, submitted.
- Fischer, M., 2012. Water Balance of Short Rotation Coppice, Ph.D Thesis. Mendel University in Brno, Brno, pp. 261.
- Foken, T., Wichura, B., 1996. Tools for quality assessment of surface-based flux measurements. *Agric. For. Meteorol.* 78, 83–105.
- Foken, T., Leuning, R., Oncley, S.R., Mauder, M., Aubinet, M., 2012. Corrections and data quality control. In: Aubinet, M., Vesala, T., Papale, D. (Eds.), *Eddy Covariance: A Practical Guide to Measurement and Data Analysis*. Springer, the Netherlands, Dordrecht, pp. 85–131.
- Foken, T., 2008. The energy balance closure problem: an overview. *Ecol. Appl.* 18, 1351–1367.
- Grip, H., Hallidin, S., Lindroth, A., 1989. Water use by intensively cultivated willow using estimated stomatal parameter values. *Hydrol. Processes* 3, 51–63.
- Guidi, W., Piccioni, E., Bonari, E., 2008. Evapotranspiration and crop coefficient of poplar and willow short-rotation coppice used as vegetation filter. *Bioresour. Technol.* 99, 4832–4840.
- Hall, R.L. et al., 1996. Hydrological effects of short rotation coppice, Technical report of Energy Technology Support Unit B/W5/00275/00/00, Harwell, UK, 226 pp.
- Hall, R.L., Allen, S.J., Rosier, P.T.W., Hopkins, R., 1998. Transpiration from coppiced poplar and willow measured using sap-flow method. *Agric. Forest Meteorol.* 90, 275–290.
- Hijmans, R.J., Cameron, S.E., Parra, J.L., Jones, P.G., Jarvis, A., 2005. Very high resolution interpolated climate surfaces for global land areas. *Int. J. Climatol.* 25, 1965–1978.
- Hlavinka, P., et al., 2011. Development and evaluation of the SoilClim model for water balance and soil climate estimates. *Agric. Water Manage.* 98, 1249–1261.
- Hlavinka, P., et al., 2015. Water balance, drought stress and yields for rainfed field crop rotations under present and future conditions in the Czech Republic. *Climate Res.* 65, 175–192.
- Horemans, J.A., Van Gaalen, H., Raes, D., Zenone, T., Ceulemans, R., 2017. Can the agricultural AquaCrop model simulate water use and yield of a poplar short rotation coppice? *Glob. Change Biol. Bioenergy* 9, 1151–1164.
- Horst, T.W., 1997. A simple formula for attenuation of eddy fluxes measured with first-order-response scalar sensors. *Boundary-Layer Meteorol.* 82, 219–233.
- Horst, T., 1999. The footprint for estimation of atmosphere-surface exchange fluxes by profile techniques. *Boundary-Layer Meteorol.* 90, 171–188.
- Hou, L.G., et al., 2010. Evapotranspiration and crop coefficient of *Populus euphratica* Oliv forest during the growing season in the extreme arid region northwest China. *Agric. Water Manage.* 97, 351–356.

- Ingwersen, J., et al., 2011. Comparison of Noah simulations with eddy covariance and soil water measurements at a winter wheat stand. *Agric. For. Meteorol.* 151, 345–355.
- Ingwersen, J., Imukova, K., Högy, P., Streck, T., 2015. On the use of the post-closure methods uncertainty band to evaluate the performance of land surface models against eddy covariance flux data. *Biogeosciences* 12, 2311–2326.
- Iritz, Z., Tourula, T., Lindroth, A., Heikinheimo, M., 2001. Simulation of willow short-rotation forest evaporation using a modified Shuttleworth–Wallace approach. *Hydrol. Processes* 15, 97–113.
- Isebrands, J.G., Richardson, J., 2014. *Poplars and Willows – Trees for Society and the Environment*. FAO&CABI, Croydon, UK, pp. 650.
- Katul, G., et al., 1999. Spatial variability of turbulent fluxes in the roughness sublayer of an even-aged pine forest. *Boundary-Layer Meteorol.* 93, 1–28.
- Kersebaum, K.C., et al., 2015. Analysis and classification of data sets for calibration and validation of agro-ecosystem models. *Environ. Modell. Software* 72, 402–417.
- Kim, H.-S., Oren, R., Hinckley, T.M., 2008. Actual and potential transpiration and carbon assimilation in an irrigated poplar plantation. *Tree Physiol.* 28, 559–577.
- King, J.S., et al., 2002. Below-ground carbon input to soil is controlled by nutrient availability and fine root dynamics in loblolly pine. *New Phytologist* 154, 389–398.
- King, J.S., et al., 2013. The challenge of lignocellulosic bioenergy in a water-limited world. *Bioscience* 63, 102–117.
- Kool, D., et al., 2014. A review of approaches for evapotranspiration partitioning. *Agric. For. Meteorol.* 184, 56–70.
- Lasch, P., Kollas, C., Rock, J., Suckow, F., 2009. Potentials and impacts of short-rotation coppice plantation with aspen in Eastern Germany under conditions of climate change. *Reg. Environ. Change* 10, 83–94.
- Liang, H., Hu, K., Batchelor, W.D., Qi, Z., Li, B., 2016. An integrated soil-crop system model for water and nitrogen management in North China. *Sci. Rep.* 6, 25755.
- Linderson, M., Iritz, Z., Lindroth, A., 2007. The effect of water availability on stand-level productivity, transpiration, water use efficiency and radiation use efficiency of field-grown willow clones. *Biomass Bioenergy* 31, 460–468.
- Lindroth, A., Båth, A., 1999. Assessment of regional willow coppice yield in Sweden on basis of water availability. *For. Ecol. Manage.* 121, 57–65.
- Lindroth, A., Iritz, Z., 1993. Surface energy budget dynamics of short-rotation willow forest. *Theor. Appl. Climatol.* 47, 175–185.
- Manca, G., 2003. *Analisi Dei Flussi Di Carbonio Di Una Cronosequenza Di Cerro (Quercus cerris L.) Dell'Italia Centrale Attraverso La Tecnica Della Correlazione Turbolenta*, Ph.D Thesis. University of Tuscia, Italy, pp. 224.
- Mauder, M., Foken, T., 2006. Impact of post-field data processing on eddy covariance flux estimates and energy balance closure. *Meteorol. Z.* 15, 597–609.
- Migliavacca, M., et al., 2009. Seasonal and interannual patterns of carbon and water fluxes of a poplar plantation under peculiar eco-climatic conditions. *Agric. For. Meteorol.* 149, 1460–1476.
- Moncrieff, J.B., et al., 1997. A system to measure surface fluxes of momentum, sensible heat, water vapour and carbon dioxide. *J. Hydrol.* 188, 589–611.
- Moncrieff, J., Clement, R., Finnigan, J., Meyers, T., 2004. Averaging, detrending, and filtering of eddy covariance time series. In: Lee, X., Massman, W., Law, B. (Eds.), *Handbook of Micrometeorology: A Guide for Surface Flux Measurement and Analysis*. Springer, the Netherlands, Dordrecht, pp. 7–31.
- Moriasi, D.N., et al., 2007. Model evaluation guidelines for systematic quantification of accuracy in watershed simulations. *Trans. ASABE* 50, 885–900.
- Novick, K.A., et al., 2016. The increasing importance of atmospheric demand for ecosystem water and carbon fluxes. *Nat. Clim. Change* 6, 1023–1027.
- Odhiambo, L.O., Irmak, S., 2012. Evaluation of the impact of surface residue cover on single and dual crop coefficient for estimating soybean actual evapotranspiration. *Agric. Water Manage.* 104, 221–234.
- Ogée, J., Brunet, Y., Loustau, D., Berbigier, P., Delzon, S., 2003. MuSICA, a CO<sub>2</sub>, water and energy multilayer, multileaf pine forest model: evaluation from hourly to yearly time scales and sensitivity analysis. *Glob. Change Biol.* 9, 697–717.
- Oren, R., et al., 1999. Survey and synthesis of intra- and interspecific variation in stomatal sensitivity to vapour pressure deficit. *Plant Cell Environ.* 22, 1515–1526.
- Peel, M.C., Finlayson, B.L., McMahon, T.A., 2007. Updated world map of the Köppen–Geiger climate classification. *Hydrol. Earth Syst. Sci.* 11, 1633–1644.
- Penman, H.L., 1948. Natural evaporation from open water, bare soil and grass. *Proc. R. Soc. A: Math. Phys. Eng. Sci.* 193, 120–145.
- Perry, C.H., Miller, R.C., Brooks, K.N., 2001. Impacts of short-rotation hybrid poplar plantations on regional water yield. *For. Ecol. Manage.* 143, 143–151.
- Persson, G., Lindroth, A., 1994. Simulating evaporation from short-rotation forest: variations within and between seasons. *J. Hydrol.* 156, 21–45.
- Persson, G., 1997. Comparison of simulated water balance for willow, spruce, grass ley and barley. *Hydrol. Res.* 28, 85–98.
- Petzold, R., Schwärzel, K., Feger, K.H., 2010. Transpiration of a hybrid poplar plantation in Saxony (Germany) in response to climate and soil conditions. *Eur. J. For. Res.* 130, 695–706.
- Raes, D., Deproost, P., 2003. Model to assess water movement from a shallow water table to the root zone. *Agric. Water Manage.* 62, 79–91.
- Raes, D., Steduto, P., Hsiao, T.C., Fereres, E., 2009. AquaCrop—The FAO crop model to simulate yield response to water: II: main algorithms and software description. *Agron. J.* 101, 438–447.
- Rawls, W., Brakensiek, D., Saxton, K., 1982. Estimation of soil water properties. *Trans. ASAE* 25, 1316–1320.
- Reichstein, M., et al., 2005. On the separation of net ecosystem exchange into assimilation and ecosystem respiration: review and improved algorithm. *Glob. Change Biol.* 11, 1424–1439.
- Rosa, R.D., et al., 2012. Implementing the dual crop coefficient approach in interactive software. 1. Background and computational strategy. *Agric. Water Manage.* 103, 8–24.
- Sánchez, N., et al., 2012. Water balance at plot scale for soil moisture estimation using vegetation parameters. *Agric. For. Meteorol.* 166–167, 1–9.
- Saxton, K.E., Rawls, W.J., Romberger, J.S., Papendick, R.I., 1986. Estimating generalized soil-water characteristics from texture. *Soil Sci. Soc. Am. J.* 50, 1031–1036.
- Schmid, H.P., 2002. Footprint modeling for vegetation atmosphere exchange studies: a review and perspective. *Agric. For. Meteorol.* 113, 159–183.
- Schmidt-Walter, P., Richter, F., Herbst, M., Schuldt, B., Lamersdorf, N.P., 2014. Transpiration and water use strategies of a young and a full-grown short rotation coppice differing in canopy cover and leaf area. *Agric. For. Meteorol.* 195–196, 165–178.
- Sheikh, V., Visser, S., Stroosnijder, L., 2009. A simple model to predict soil moisture: bridging Event and Continuous Hydrological (BEACH) modelling. *Environ. Modell. Software* 24, 542–556.
- Shuttleworth, W.J., 2007. Putting the vap into evaporation. *Hydrol. Earth Syst. Sci.* 11, 210–244.
- Stannard, D.I., 1997. A theoretically based determination of Bowen-ratio fetch requirements. *Boundary-Layer Meteorol.* 83, 375–406.
- Stanturf, J.A., Oosten, C. v. Netzer, D.A., Coleman, M.D., Portwood, C.J., 2001. Ecology and silviculture of poplar plantations. In: Dickmann, D.I., Isebrands, J.G., Eckenwalder, J.E., Richardson, J. (Eds.), *Poplar Culture in North America*. NRC Research Press, Ottawa, Canada, pp. 153–206.
- Steduto, P., Hsiao, T.C., Raes, D., Fereres, E., 2009. AquaCrop—The FAO crop model to simulate yield response to water: I. concepts and underlying principles. *Agron. J.* 101, 426–437.
- Trnka, M., et al., 2008. Biomass production and survival rates of selected poplar clones grown under a short-rotation system on arable land. *Plant Soil Environ.* 54, 78–88.
- Trnka, M., et al., 2010. Simple snow cover model for agrometeorological applications. *Agric. Forest Meteorol.* 150, 1115–1127.
- Trnka, M., et al., 2016. Potential and limitations of local tree ring records in estimating *a priori* the growth performance of short-rotation coppice plantations. *Biomass Bioenergy* 92, 12–19.
- Twine, T.E., et al., 2000. Correcting eddy-covariance flux underestimates over a grass-land. *Agric. For. Meteorol.* 103, 279–300.
- van Dijk, A.I.J.M., et al., 2015. Rainfall interception and the coupled surface water and energy balance. *Agric. Forest Meteorol.* 214–215, 402–415.
- Vanbever, S.P., et al., 2016. A comparative study of four approaches to assess phenology of *Populus* in a short-rotation coppice culture. *iForest – Biogeosci. For.* 9, 682–689.
- Verlinden, M.S., Broeckx, L.S., Ceulemans, R., 2015. First vs. second rotation of a poplar short rotation coppice: above-ground biomass productivity and shoot dynamics. *Biomass Bioenergy* 73, 174–185.
- Webb, E.K., Pearman, G.I., Leuning, R., 1980. Correction of flux measurements for density effects due to heat and water vapour transfer. *Q. J. R. Meteorol. Soc.* 106, 85–100.
- Williams, R., Ahuja, L., 1993. Using available water content with the one-parameter model to estimate soil water retention. *Soil Sci.* 156, 380–388.
- Willmott, C.J., 1982. Some comments on the evaluation of model performance. *Bull. Am. Meteorol. Soc.* 63, 1309–1313.
- Wilson, K., et al., 2002. Energy balance closure at FLUXNET sites. *Agric. For. Meteorol.* 113, 223–243.
- Yang, D., et al., 1998. Accuracy of NWS 8 standard nonrecording precipitation gauge: results and application of WMO intercomparison. *J. Atmos. Oceanic Technol.* 15, 54–68.
- Zenone, T., et al., 2015. Biophysical drivers of the carbon dioxide, water vapor, and energy exchanges of a short-rotation poplar coppice. *Agric. For. Meteorol.* 209–210, 22–35.
- Zenone, T., et al., 2016. Interaction between isoprene and ozone fluxes in a poplar plantation and its impact on air quality at the European level. *Sci. Rep.* 6, 32676.
- Zenone, T., 2007. *Measuring Terrestrial CO<sub>2</sub> Uptake in a Short Rotation Forestry of Poplar for Bioenergy Production: Comparison Between Biometric and Micrometeorological Technique*, Ph.D Thesis. University of Padova, Italy, pp. 105.